A Bushveld-related high-Ti igneous suite (HITIS) derived from an alkali to transitional basaltic magma, South Africa

Sybrand de Waal
Centre for Research on Magmatic Ore Deposits, Department of Geology,
University of Pretoria, Pretoria 0002, South Africa.
Current address: PO Box 21167, Windhoek, Namibia
e-mail: heimat@iway.na (corresponding author)

Joachim-Klaus Schweitzer
Department of Geology, University of Pretoria, Pretoria, 0002 South Africa.
Current address: Shango Solutions, HHK House, Cnr. Ethel Road and Ruth Crescent, Northcliff
e-mail: jochen@shango.co.za

Ian Graham
Centre for Research on Magmatic Ore Deposits, Department of Geology,
University of Pretoria, Pretoria 0002, South Africa.
Current address: School of Biological, Earth and Environmental Sciences
University of New South Wales Sydney, New South Wales, 2052 Australia
e-mail: i.graham@unsw.edu.au

Christoph Gauert
Department of Geology, University of Pretoria, Pretoria, 0002 South Africa.
Current address: Department of Geology, University of the Free State, Bloemfontein, South Africa
e-mail: gauertcdk.sci@mail.uovs.ac.za

Edward Ripley
Department of Geological Sciences, Indiana University, Bloomington, IN 47405, United States of America
e-mail: ripley@indiana.edu

ABSTRACT

A suite of high-Ti mafic to felsic igneous rock (acronym: HITIS) was emplaced at ~2055 Ma as km-sized bodies to the south of the Bushveld Complex, South Africa, stretching from Parys and Potchefstroom in the south-west to Marble Hall in the north and Badplaas in the east. Currently known members of the suite include the Marble Hall sills and related intrusives and breccia, the Basal Gabbro Unit of the Uitkomst Complex, the Lindeques Drift and Heidelberg intrusions, the volcanic Roodekraal Complex, the Rietfontein Complex, the Koedoesfontein Complex, the Schoongezicht (previously Kaffirskraal) Complex, the Vredefort alkali granite, as well as the high-Ti basalt and FeTiP-enriched basaltic lava of the Rooiberg Group. The volcanic rocks extruded on mildly folded and denuded metasedimentary rocks and lava of the Pretoria Group, whereas the plutonic rocks intruded at a level between the upper Witwatersrand Supergroup and the lower Pretoria Group, but largely within the dolomite of the Chuniespoort Group. The mafic rocks in this suite are dominated by clinopyroxene (salite to augite), FeTi-oxide (magnetite-ilmenite), amphibole (largely edinitic and hastingsitic), olivine (Fo_{44} to Fo_{80}), orthopyroxene and plagioclase ($An_{<50}$), forming an array of dioritic and subordinate gabbroic rocks with associated clinopyroxene±magnetite(-ilmenite)±olivine±plagioclase cumulates. Locally, hybrid calc-silicate rocks derived from reaction of the magma with dolomite of the Chuniespoort Group are developed. The felsic rocks are syenodiorite and alkali granite with K-feldspar, albite, alkali pyriboles and biotite. Trace element systematics suggests that the HITIS rocks are derived from an alkali to transitional basaltic parent. The most primitive rocks representing liquid fractions are developed in the chill zone of the Basal Gabbro Unit of the Uitkomst Complex (Mg# 0.55 to 0.68) and in the Marble Hall diorite sills (Mg# = 0.53 to 0.65). These are followed by the more evolved high-Ti basalt (Mg# = 0.45 to 0.50) of the Rooiberg Group, the mugearite lavas (Mg# = 0.29 to 0.47) of the volcanic Roodekraal Complex, the FeTiP lava (Mg# = 0.17 to 0.30) of the Rooiberg Group, and finally the Vredefort alkali granite (Mg# = 0.26 to 0.72). This rock series resulted from deep-seated (lower crustal?) amphibole fractionation, followed by shallow level clinopyroxene±magnetite(-ilmenite)±olivine±plagioclase fractionation with the FeTi-oxide phases becoming more dominant in the later stages. The Vredefort alkali granite represents the final liquid in the liquid line of descent. The HITIS magma marks an early stage in the Bushveld magmatic event and has a close temporal relationship with the boninitic B1-type magma, regarded as parental to the Lower Zone of the Bushveld Complex. It also appears to have been derived from the same mantle source that yielded the tholeiitic B3-type magma, which is in part responsible for the Main Zone of the Bushveld Complex. Minor copper and PGE concentrations are associated with cumulate rocks of the HITIS.

SOUTH AFRICAN JOURNAL OF GEOLOGY, 2008, VOLUME 111 PAGES 201-224
doi:10.2113/gssajg.111.2-3.201

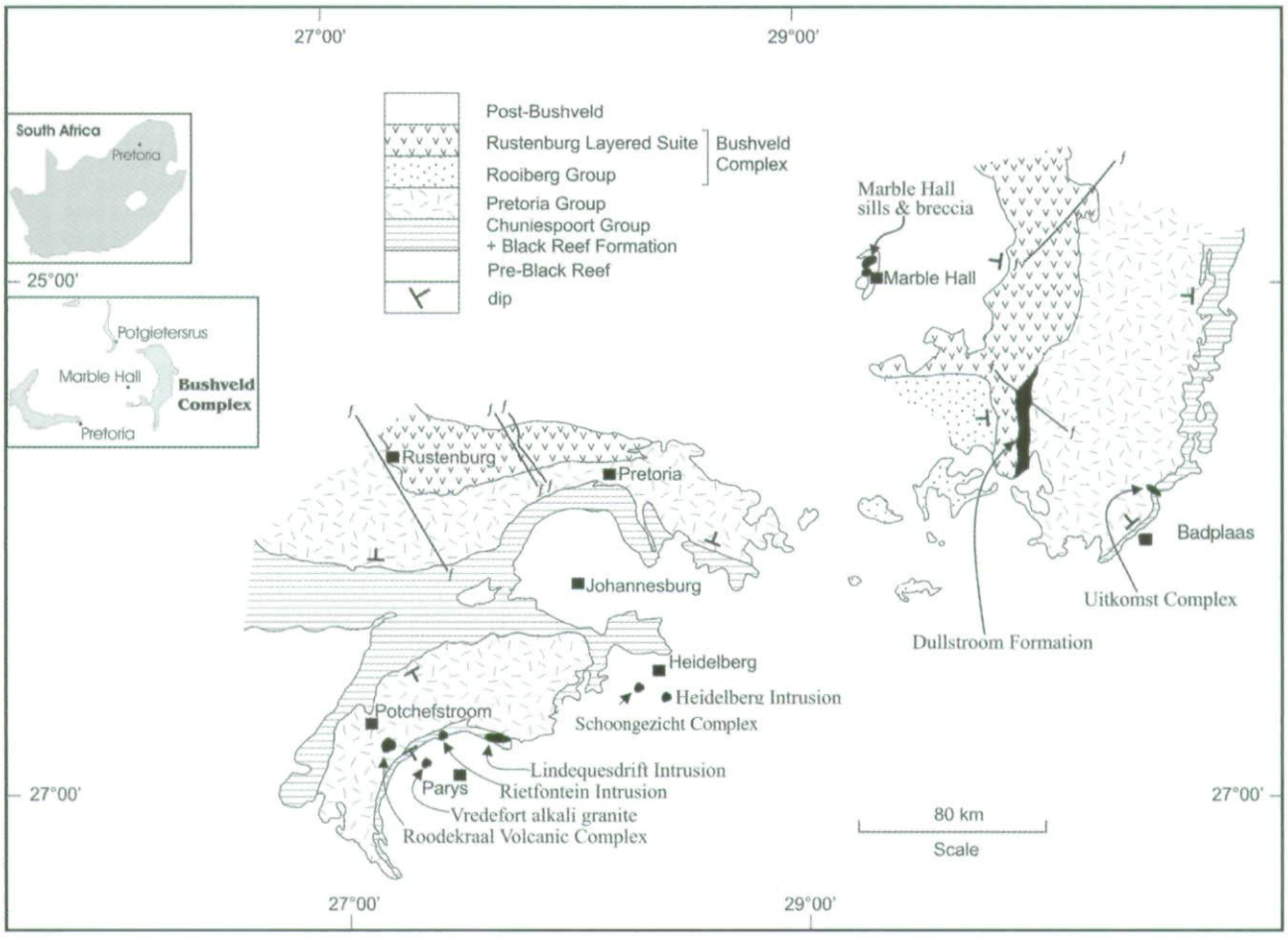

Figure 1. Geographic distribution of the HITIS rocks.

Introduction

The Bushveld Complex in South Africa comprises three major lithological units. The volcanogenic Rooiberg Group (2061 ± 2 Ma; Walraven, 1997), composed of acid lava with subordinate mafic lava near its base (Schweitzer *et al.*, 1995), extruded unconformably on a floor of mildly folded and denuded rocks of the Transvaal Supergroup (approximately 2.6 to 2.2 Ga; Armstrong *et al.*, 1991). The Rustenburg Layered Suite (RLS) is a sequence of ultrabasic to basic cumulate rocks (Eales, 2002, and references therein), that intruded as extensive sill-like bodies, roughly following the unconformity at the base of the Rooiberg Group (Cheney and Twist, 1991). Finally, A-type granite of the Lebowa Granite Suite (2054 ± 2 Ma; Walraven and Hattingh, 1993) was emplaced as a thick compound sheet roughly at the contact of the RLS with the overlying Rooiberg Group.

Geochemical studies (Harmer and Sharpe, 1985; Sharpe, 1981; 1984; 1985; Kruger, 1994; Hatton, 1988; Cawthorn *et al.*, 1981; Davies *et al.*, 1980; Davies and Tredoux, 1985), as summarized by Eales (2002), suggest that at least five different parental magma types contributed to the RLS. Cumulates of the B1-type (U-magma), a high-Mg andesite, constitute the Lower Zone and lower Critical Zone. Tholeiitic B2-, B3- and B4-type magmas (A-magmas) yielded the cumulates of the upper Critical, Main and Upper Zones, respectively. A fifth magma is postulated to explain the strong chemical reversals at the level of the Pyroxenite Marker at the base of the Upper Zone (Davies and Cawthorn, 1984).

Less well appreciated until now is the existence of a high-Ti igneous suite of mafic to felsic rocks (acronym: HITIS), referred to earlier by De Waal and Armstrong (2000) and De Waal and Theart (2004), which outcrop as relatively small (km-sized) bodies scattered over a total area of approximately 20 000 km^2 (Figure 1). A quadrangle defined by lines connecting Potchefstroom and Parys in the southwest, Badplaas in the east, and Marble Hall in the north roughly contains all the currently known occurrences of HITIS rocks. The suite includes the Marble Hall sills and related intrusives and breccia bodies, the Basal Gabbro Unit of the Uitkomst Complex, the Lindeques Drift and Heidelberg Intrusions, the volcanic Roodekraal Complex, the Rietfontein Complex, the Koedoesfontein Complex, the Schoongezicht (previously Kaffirskraal) Complex, the Vredefort alkali granite, as well as the high-Ti basalt and FeTiP basaltic lava of the Rooiberg Group.

In this paper we review the petrology and geochemistry of the HITIS and show that, although it has a close temporal relationship with the B1-type magma, it is derived from an alkali to transitional basaltic magma. The latter, which is the Bu magma of De Waal and

Gauert (1997) and De Waal and Armstrong (2000), evidently represents a low fraction mantle melt from the same source as the Bushveld B3-type magma. Fractionation of the Bu magma at different levels in the crust yielded a derivative ferrobasalt that is parental to the Lindeques Drift and Heidelberg Intrusions as well as the Roodekraal Complex (De Waal *et al.*, 2005), and finally the Vredefort alkali granite. We also underscore the observation of Graham *et al.* (2005) that the Bushveld magmatic activity extended towards the Vredefort Dome way beyond the current outcrop area of the RLS. This activity may explain the high heat flow regime just prior to impact reported from the Vredefort area by earlier workers (Gibson and Reimold, 2001, and references therein).

Methods of investigation

This paper is in part based on published information and the reader is referred to the relevant publications for the methods of investigation used by the different authors. The descriptions that follow here apply only to the new data added during this study.

Thin and polished thin sections were investigated with an optical microscope. Selected mineral grains were analysed on a Cameca SX100 electron microprobe at the Department of Geology, University of Pretoria. Counting times on peak positions were 20 seconds, and 10 seconds on each background positions. The electron beam was defocused to a 10 micron diameter for feldspar. Wollastonite was used as standard for Si and Ca, pure oxides for Mg, Al, Mn, Cr, Ti, Ni, Fe, orthoclase for K, albite for Na, tugtupite for Cl, and fluorite for F. A ZAF correction procedure was applied throughout.

Selected samples were analyzed for major and trace elements on an ARL 8420 wavelength-dispersive XRF spectrometer in the XRF/XRD Laboratory of the Department of Geology, University of Pretoria. Samples were dried and roasted at 950°C to determine percentage loss on ignition (LOI). Major-element analyses were performed on fused beads, following a standard method adapted from Bennett and Oliver (1992). One gram of pre-roasted sample is mixed with 6g lithium tetraborate flux in a 5% Au/Pt crucible, and fused at 1050°C in a muffle furnace with occasional swirling. Glass disks were poured into a pre-heated Pt/Au mould, with the bottom surface presented for analysis. The samples were analyzed for selected trace elements on pressed powder pellets with saturated Movial solution as binder, using an adaptation of the method described by Watson (1996). The XRF spectrometer was calibrated with certified reference materials. The NBSGSC fundamental parameter program was used for matrix correction for the major elements as well as of Cl, Co, Cr, V, Ba and Sc. The Rh Compton peak ratio method was used for the other trace elements.

The platinum-group elements, Re, Ni, Cu and Au of selected samples were determined by instrumental neutron activation analysis (INAA) at the University of Quebec at Chicoutimi (UQAC). Details of the method are given in Bédard and Barnes (2002).

Rare Earth and selected trace elements were analyzed at the Department of Earth Sciences, University of Cape Town. 50 mg sample aliquots were dissolved by a standard acid digestion procedure using ultra-clean HF and HNO_3. Calibration was made using external synthetic multi-element standards. The samples were then analyzed using a Perkin Elmer/Sciex Elan 6000 ICP-MS. Internal standardization was achieved using 103Rh, 115In, 187Re and 209Bi. Typical detection limits for all the rare earth elements are in the ppt-range. Each sample solution was analyzed in triplicate, with 20 sweeps per replicate, and the data quoted represent average values of these duplicate analyses. Both the within-run and duplicate analysis precision was mostly between 2% relative and always better than 3% relative (1 sigma).

Selected samples were analyzed for S isotopic ratios in the Department of Geological Sciences of the Indiana University, Bloomington, Indiana, United States of America. Five to 10 mg powder samples of whole-rock samples were loaded in tin capsules along with approximately 1mg of V_2O_5. The capsule was then flash combusted in an oxygen stream using a Carlo Erba elemental analyser. The produced SO_2 was passed through an oxidation-reduction reactor at 1010°C and a GC column prior to entering the Finnigan MAT 252 mass spectrometer. Measurements were made using continuous flow isotopic ratio monitoring methods with a He carrier gas. The results are reported relative to VCDT with an analytical precision of +/- 0.1 ‰ (though normally less).

The calculation of partition coefficients to test fractionation models involves the determination of the slopes of the lines described by the variation in the log concentration of a given trace element, x, against that of Ce, in a binary diagram. These slopes are numerically equal to

$$[D_x^{(A/liquid)} -1]/ [D_{Ce}^{(A/liquid)} -1]$$

where D_{Ce} and Dx are the bulk partition coefficients for Ce and element x, and A refers to the fractionating phase(s). For a slope = $K_{(x,Ce)}$

$$D_x^{(A/liquid)} = K_{(x,Ce)} D_{Ce}^{(A/liquid)} -K_{(x,Ce)} +1$$

This relationship allows the calculation of the partition coefficient for any number of trace elements, provided $D_{Ce}^{(A/liquid)}$ is known. The latter can be estimated from published values for a given fractionation model, and if the model approaches reality then all the calculated D_x's should approximate the published D_x's for the given model. It stands to reason that high accuracy analytical data, typically obtained by ICP-MS, coupled with high quality published D values best suit this approach.

The addition-subtraction method discussed by Rollinson (1993) was used to determine the composition

of the fractionating phases in the different stages of development of the HITIS liquid. This method involves the identification of a conserved component (element oxide, incompatible trace element), *i.e.* a component that did not fractionate during the given stage of differentiation. If A_1 and A_2 are the starting and final concentrations of a fractionating component in a given fractionation stage, and B_1 and B_2 the starting and final concentrations of the conserved component in the same stage, the concentration of the fractionating component, A_3, in the fractionating solid is given by

$$A_3 = A_1 - m^*B_1 = A_2 - m^*B_2$$

where $m = (A_1 - A_2)/(B_1 - B_2)$, which is the rate of change of A relative to B in the given stage. By repeating this calculation for each element oxide an estimate of the chemical composition of the fractionating solids can be obtained. The accuracy of the method hinges strongly on the accuracy of analytical data. Least squares minimization techniques can then be applied to recalculate the chemical compositions of the fractionating solids into mineral norms using mineral compositions from the relevant rock suite.

Nomenclature and abbreviations

In this paper we use the word 'liquid' to refer to rock melt that experienced no net gain of any of the fractionating phases during crystallization. Rocks that represent melt with a net gain of a fractionating phase are referred to as 'cumulates'. The chemical compositions of the sequence of residual liquids formed by continual loss of fractionation products define the 'liquid line of descent'.

The following abbreviations are used in the tables and figures, and if convenient, also in the text:

Ab - albite
Ac - acmite
Amph - amphibole
An - anorthite
BGU - Basal Gabbro Unit
Cmlts - cumulates
Cpx - Ca-rich clinopyroxene
CZ - chill zone
Di - diopside
En - enstatite
Fa - fayalite
Fe_2O_3T - total Fe as Fe_2O_3
Fo - forsterite
Fs - ferrosilite
Gt - garnet
Hd - hedenbergite
HI - Heidelberg Intrusion
Il - ilmenite
KC - Schoongezicht Complex
Kfsp - K-feldspar
LI - Lindeques Drift Intrusion
MH - Marble Hall
Mt - magnetite
Ol - olivine
Opx - orthopyroxene
Plag - plagioclase
RC - Roodekraal Complex
RG - Rooiberg Group
RietC - Rietfontein Complex
Tvl - Transvaal Supergroup
UC - Uitkomst Complex
UM - ultramafic
Ven - Ventersdorp Supergroup
Wo - wollastonite
WWR - Witwatersrand Supergroup

Distribution, field relations and absolute age

Marble Hall sills and breccia

The Marble Hall Fragment (Figure 1), situated 120 km northeast of Pretoria, is an intensely folded, dome-like, inlier of supracrustal rocks of the Transvaal Supergroup in Nebo Granite of the Bushveld Complex (De Waal *et al.*, 2002; De Waal and Armstrong, 2000; De Waal, 1969; 1963; Snyman, 1958). The Fragment is pear-shaped measuring about 30 km along a northeast-southwesterly direction and about 20 km across. Recently, Babayeju (1999) used gravity and total field magnetic data to show that the Fragment is a horst block of floor rocks of the Bushveld Complex that protrude through the current level of the RLS. This interpretation complements the work of Hattingh (1980), who contended that the eastern compartment of the RLS abuts in depth against the eastern side of the Marble Hall Fragment.

Dioritic rocks, dated at 2056 ± 3 Ma (SHRIMP zircon $^{207}Pb/^{206}Pb$; De Waal and Armstrong, 2000) form scattered outcrops on the farms Scherpe Arabie 116, Rooibokkop 491, Uyskraal 228 and Elandsdrift 117 in the central part of the Marble Hall Fragment north and west of the town of Marble Hall. South of Marble Hall, comparable dioritic rocks were encountered in a deep borehole (borehole LD2, De Waal and Armstrong, 2000; De Waal *et al.*, 2002), where they form a 338 m-thick multiple sill complex, below a ~186 m thick cover of Malmani dolomite. The sills are sub-horizontal and cut discordantly over the intensely folded dolomite, and shale and quartzite of the Pretoria Group.

More massive diorite bodies (sills?) at Marble Hall are differentiated. The LN2 body (Graham *et al.*, 2004), situated about 3.4 km due south of Marble Hall, was intersected in a borehole (LN2). It comprises cumulate diorite overlain by a diorite pegmatite cap rock and underlain by calc-silicate hybrid rocks. The latter represent products of reaction between the diorite magma and the carbonate country rock. Approximately 1.1 km south of the town, another massive body of ultramafic rock was intersected in a borehole (LN1). The shape and lateral extent of this body, here referred to as the LN1 body, is unknown. Babayeju (1999) showed the presence of a large positive gravity anomaly centred around the town of Marble Hall and the LN1 body could conceivably contribute to this anomaly.

Melagabbronorite was observed as a meter-sized dyke-like intrusion on Rooibokkop 491 (De Waal, 1963), near the northern extremity of the Marble Hall Fragment. The country rock at this locality is thermally metamorphosed to the hornblende hornfels facies (De Waal, 1963, 1969) and the melagabbronorite displays granoblastic features suggestive of thermal metamorphism.

Large bodies of monomictic and polymictic breccia (2055.6 ± 3.1 Ma, $^{40}Ar/^{39}Ar$; De Waal *et al.*, 2002), associated with the diorite, are interpreted to be the result of volatile build-up and explosive venting of some of the diorite sills. These breccias in places contain fragments of Bushveld B1-type sill rocks (De Waal *et al.*, 2002), suggesting the B1 magma to predate the formation of the breccia bodies.

Basal Gabbro Unit of the Uitkomst Complex

The Uitkomst Complex (Figure 1) is located approximately 200 km due east of Pretoria on the farms Uitkomst 541JT and Slaaihoek 540JT. It is a small, tubular Ni-Cu-Cr-PGE-mineralized layered intrusion measuring 0.75 by 1.2 by 12+ km (Gauert, 1998, Gauert *et al.*, 1995; Strauss, 1995), and it hosts the only primary nickel mine in South Africa. The Complex intruded the Transvaal Supergroup at a level between the Oaktree Formation (2549 ± 2.6 Ma; Walraven and Martini, 1995) and the Klapperkop Quartzite member of the Timeball Hill Formation. The intrusion plunges at 6 to 8° to the northwest and was subdivided (Gauert *et al.*, 1995) into six units, *i.e.*, from bottom to top, the Basal Gabbro (BGU), Lower Harzburgite, Chromitiferous Harzburgite, Main Harzburgite, Pyroxenite and Gabbronorite Units. De Waal *et al.* (2001) reported a SHRIMP zircon $^{207}Pb/^{206}Pb$ age of 2044 ± 8 Ma for a diorite from the Gabbronorite Unit.

The BGU (up to 12 m thick) is a sill-like intrusion at the base of the Lower Harzburgite (Gauert *et al.*, 1995; Strauss, 1995), which in places extends laterally into the country rock beyond the limits of the main trough. It has a well-developed aphanitic chill zone (Gauert *et al.*, 1995; Agranier, 2000) against the floor rocks and a gradational contact with the overlying ultramafic rocks (De Waal *et al.*, 2001; Gauert, 1998), suggesting an age of emplacement close to or pre-dating that of the overlying units. The BGU is chemically distinct from the five upper units, the latter having Bushveld B1-type magma as parent (De Waal *et al.*, 2001).

Lindeques Drift Intrusion

The Lindeques Drift Intrusion (De Waal *et al.*, 2005; Bisschoff, 1972) is situated approximately 130 km south-southwest of Pretoria (Figure 1) on the farms Oorbietjesfontein 20, Woodlands 192, Boschdraai 33 and Vaaldraai 277. It is essentially a sill of even-grained to porphyritic spessartite (De Waal *et al.*, 2005) with an estimated thickness of ca. 150 to 200 m, outcropping over a strike length of 11 km. Dykes and sills of medium- to fine-grained diorite and syenodiorite crosscut the spessartite.

The Intrusion was emplaced in dolomite of the Malmani Subgroup, Chuniespoort Group (2549 ± 2.6 Ma, U/Pb evaporation; Walraven and Martini, 1995) of the Transvaal Supergroup, and is cut by pseudotachylite veins related to the Vredefort impact event (2023 ± 4 Ma; Kamo *et al.*, 1996). Recent SHRIMP zircon $^{207}Pb/^{206}Pb$ dating of the spessartite by De Waal *et al.* (2005) gave an age of 2054.8 ± 5.7 Ma.

Heidelberg Intrusion

The Heidelberg Intrusion sub-outcrops underneath a 45 meter thick cover of Karoo rocks on the farm Elandsfontein 412 ER in the Heidelberg District, about 95 km south of Pretoria and 12 km southeast of the Schoongezicht Complex. The shape and lateral extent of the intrusion is not known. The country rock (quartzite and shale) most likely belongs to the Turffontein Subgroup of the Central Rand Group. The predominating rock in the Heidelberg Intrusion (De Waal *et al.*, 2005) is spessartite, which is intruded by narrow dykes of alkali granite.

Roodekraal Complex

The Roodekraal Complex (De Waal *et al.*, 2005; Bisschoff, 1972; Clark, 1972) forms a series of low hills 10 km south of Potchefstroom on the farms Roodekraal 37, Plessiskraal 43 and Prinsloosrust 93. The Complex is slightly oblong with a northeast-striking long axis of about 6 km. It sits unconformably on tilted quartzite, shale and Hekpoort lava (2224 ± 21 Ma; Rb-Sr; Burger and Coertze, 1973) of the Pretoria Group. The Complex has a crude concentric morphology with an outer rim of mugearitic lava (De Waal *et al.*, 2005), a central zone of medium- to coarse-grained diorite and an intermediate zone of fine-grained diorite (Bisschoff, 1972). The diorite represents sill intrusions below the initial lava pack. A quench-textured diorite was dated at 2053.9 ± 9.2 Ma (SHRIMP zircon $^{207}Pb/^{206}Pb$; De Waal *et al.*, 2005). The Roodekraal rocks are cut by pseudotachylite related to the Vredefort impact event.

Rietfontein Complex

Bisschoff (1969; 1999) describes the Rietfontein Complex (Figure 1), on the farms Rietfontein 446 and 447, as two poorly exposed elongated bodies consisting of mafic to ultramafic rocks (southern section) and alkali granite (northern section) and covering a total area of about 18 square km. The Complex intruded the upper lava of the Ventersdorp Supergroup, quartzite of the Black Reef Formation and dolomite of the Chuniespoort Group. The latter formations are overturned and dip at 25 to 70° to the southeast. Outcrops are poor, but Bisschoff (1969) showed that the mafic-ultramafic portion is dominated by wehrlite, troctolite, spessartite, olivine gabbro and picrogabbro. Dips in the latter rocks are 75 to 80° to the north. The poor outcrops preclude any inference on the shape of the Complex.

The Complex postdates the Chuniespoort Group (2549 ± 2.6 Ma; Walraven and Martini, 1995) and

predates (Bisschoff, 1969) the Vredefort impact event (2023 ± 4 Ma; Kamo *et al.*, 1996). In addition, the close association of the mafic-ultramafic rocks with alkali granite, petrographically comparable to that at Baviaanskrantz (Graham *et al.*, 2005), 15 km to the southwest (Figure 1), suggests a magmatic co-lineage with the Lindequest Drift, Heidelberg and Vredefort alkali granite intrusions.

Schoongezicht (previously Kaffirskraal) Complex

The Schoongezicht Complex (Frick, 1975, 1979; Nel and Jansen, 1957) is located 90 km due south of Pretoria on the farms Kaffirskraal 381 and Schoongezicht 378. The Complex, which intruded lava of the Ventersdorp Supergroup, is oval-shaped measuring 1.8 km in a north-easterly direction and 0.95 km across. A steeply inward dipping (70°) outer marginal zone of porphyritic norite (1 m thick) is followed upward by a layered magnetite clinopyroxenite. The latter, which makes up the bulk of the body, is layered and dips at 4° towards the centre of the Complex. The magnetite clinopyroxenite is interlayered with feldspathic pyroxenite, magnetite dunite and magnetite wehrlite. A magnetitite layer (8 m thick) caps the magnetite clinopyroxenite. The rocks clearly represent the lower part of a larger body, the upper sequences of which have been removed by erosion.

Xenoliths of quartzite, hornfels, gabbro and norite are contained in the magnetite clinopyroxenite. Nel and Jansen (1957) regarded the gabbro and norite inclusions to be derived from mafic sills in the underlying Witwatersrand Supergroup, whereas Frick (1975) saw it as related to the Complex. Evidence to be presented later in this paper suggests these gabbroid rocks to be highly altered calc-silicate xenoliths.

High-Ti and FeTiP lavas

Schweitzer *et al.* (1995) reviewed the distribution and lithogeochemistry of the Rooiberg Group and subdivided it into the Dullstroom, Damwal, Kwaggasnek and Schrikkloof Formations (from stratigraphic bottom to top). Of these, the Dullstroom Formation is lithologically the most complex in that it represents five different magma types, *i.e.* FeTiP basalt, high-Ti basalt, low-Ti basalt-andesite, high-Mg rhyolite and basal rhyolite. The first two types of magma are regarded as members of the HITIS. The high-Ti basalt is restricted to the Bothasberg area, whereas the high-FeTiP lava is found in the Loskop Dam and Stoffberg areas (Schweitzer *et al.*, 1995). Rhyolite from the Kwaggasnek Formation was dated at 2061 ± 2 Ma (Pb evaporation on zircon; Walraven, 1997).

In this paper we ignored the 'high silica' members of the high-Ti lava. These rocks are enriched in patchily developed and microscopically visible quartz and show a large amount of chemical scatter. The source of the quartz is not apparent and a detailed investigation into its origin is beyond the scope of this paper.

Vredefort alkali granite

The Vredefort alkali granite includes the Baviaankranz and Schurwedraai alkali granite as well as numerous smaller bodies associated with the mafic rocks of the HITIS. The Baviaankranz and Schurwedraai plutons (Elsenbroek, 1991; 1993) are situated approximately 150 km southwest of Pretoria (Figure 1) on the farms Schurwedraai 382, Barnardsrust 1003, Boomplaas 1005, Koedoeslaagte 516 IQ, Hydochs Rust 466, Baviaankranz 436, Heuningsrust 970, Goedgedag 971, Elisa 972 and Helena 780. The granite forms two elongated outcrops, the Schurwedraai and Baviaanskranz plutons, each 3 to 4 km in length and trending roughly northeasterly (Elsenbroek, 1991; 1993), as well as a few smaller scattered occurrences. The granite intruded shale and quartzite of the Witwatersrand Supergroup. Graham *et al.* (2005) dated the Baviaanskranz pluton at 2052 ± 14 Ma (SHRIMP zircon $^{207}Pb/^{206}Pb$).

Alkali granite is also associated with the Rietfontein Complex (Bisschoff, 1969), the Koedoesfontein Complex (Bisschoff, 1969) and the Heidelberg Intrusion (De Waal *et al.*, 2005)

Other smaller intrusions

Bisschoff (1969; 1999) reported relatively small outcrops of spessartite and wehrlite on the farm Koedoesfontein 12 and spessartite on Koppieskraal 89. These rocks are petrographically comparable to those in the Rietfontein Complex and Lindeques Drift Intrusion and most probably also belong to the HITIS. However, due to limited information they will only be given a cursory treatment in this paper.

Petrography

Marble Hall sills and breccia

The dioritic rocks at Marble Hall (De Waal and Armstrong, 2000) range from a melagabbronorite (14% MgO) through meladiorite (6.7 to 9% MgO) and diorite (~2 to 6.7% MgO), to leucodiorite and sodic anorthosite (<2% MgO). The diorite, which forms the bulk of the rocks, typically is fine- to medium-grained consisting essentially of clinopyroxene, brown to green amphibole, plagioclase, brown biotite, magnetite(-ilmenite), apatite, K-feldspar, minor quartz and zircon as primary magmatic minerals. The clinopyroxene ($Wo_{44}En_{41}Fs_{13}Ac_2$) generally forms stubby idiomorphic prisms (ca. 1 mm across) ranging up to 30 modal per cent, and, as a rule, is partly replaced by the amphibole. Brown hastingsitic and edenitic amphibole (~20 to 55 modal %) reacted with and partly replaced clinopyroxene and plagioclase in the late magmatic stage. The brown amphibole is rimmed by green magnesio-hornblende, actinolite and ferro-actinolite, reflecting the reduced temperature towards the later stages of crystallization. Plagioclase (mostly $An_{<48}$; ~20 to 70 modal %) is compositionally zoned with the core areas highly saussuritized suggesting originally higher anorthite contents. Plagioclase shows a sub-ophitic relationship with the pyribole aggregates, largely

as a result of the late stabilization of amphibole. Rare olivine (Fo_{44-49}), with wide reaction rims, was observed in some sections. The K-feldspar and quartz represent late phases filling interstices between early minerals in the more evolved diorite. The paragenetic sequence in the diorite is: clinopyroxene-plagioclase-amphibole-magnetite(-ilmenite)-apatite-biotite-quartz, with some degree of overlap between plagioclase, amphibole, magnetite(-ilmenite) and apatite. Secondary phases include saussurite, chlorite, calcite, sphene, epidote and scapolite.

The diorite of the LN2 body (Graham *et al.*, 2004) essentially is an amphibole(-clinopyroxene) cumulate that consists of sodic plagioclase (60 to 70 modal %), amphibole (15 to 25 modal %), biotite (<12 modal %), apatite (<3 modal %), chlorite (<3 modal %) and opaque minerals (<7 modal %), along with accessory sphene, zircon and calcite. The amphibole, which sporadically contains cores of clinopyroxene ($Wo_{46}En_{37}Fs_{16}Ac_1$), is commonly zoned and acicular in a matrix of interlocking grains of plagioclase. The amphibole needles display a well-developed planar fabric in a sub-horizontal plane. Diorite pegmatite with plagioclase (~85 modal %), fine-grained actinolite-ferroactinolite (~10 modal %), chlorite and apatite forms a cap rock on the diorite.

A hybrid rock is developed between the diorite of the LN2 body and the carbonate floor rock (Graham *et al.*, 2004). It varies widely in texture and composition from sample to sample, and consists of variable amounts of amphibole, biotite, olivine (Fo_{82}), serpentine, diopsidic clinopyroxene, green spinel, talc, sphene, zoisite, chlorite, zircon and calcite, along with accessory apatite and opaque phases (pyrrhotite, magnetite, ilmenite). Amphibole varies from pargasitic hornblende through pargasite to actinolite on the outer rims of the crystals.

In the meladiorite (MgO > ~6.7%) from Marble Hall, clinopyroxene becomes a distinct cumulus phase and, in conjunction with late magmatic amphibole may reach concentrations of about 35 modal per cent (*e.g.* X600). In some samples, magnetite(-ilmenite) aggregation (<5 modal %) is observed.

The melagabbronorite (X514) has a fine-grained blastopoikilitic texture, consisting of clinopyroxene (38 modal %), brown amphibole (30 modal %), orthopyroxene (13 modal %) and plagioclase (An_{55}, 18 modal %) with minor opaque oxides (<2 modal %), biotite and secondary chlorite veins. The orthopyroxene forms large (<3 mm diameter) poikilitic crystals that enclose equant crystals (~0.1 to 0.15 mm in diameter) of clinopyroxene, plagioclase and amphibole. Typical dihedral angles of 120° between the latter three major minerals indicate metamorphic recrystallization, which is in line with field evidence. The poikilitic texture is seen as an igneous relict and the amphibole apparently replaced early-formed clinopyroxene and plagioclase before the metamorphic event.

Polymictic and monomictic breccia bodies north of Marble Hall (De Waal *et al.*, 2002) contain angular fragments of country rock including marble, diopside fels, chert, adinole, Bushveld B1-type sill rock, scapolitized diopside-amphibole-plagioclase-sphene-zircon fels and scapolite-amphibole-diopside-sphene fels. The polymictic breccia typically has actinolite amphibole and albitic plagioclase in its groundmass, whereas almost pure pargasitic amphibole forms the matrix in the monomictic breccias. The amphibole in the latter grew from the walls of open fractures, squeezing out the remaining feldspar-enriched melt to leave only a narrow zone of plagioclase-bearing rock along a central parting in the fracture fills.

Ultramafic rocks encountered in the LN1 body are olivine cumulates. Intercumulus phases are clinopyroxene, saussuritized plagioclase, brownish phlogopite as well as minor sulphide and chrome spinel. Amphibole replaces pyroxene, and secondary magnetite and greenish phlogopite are common.

Basal Gabbro Unit of the Uitkomst Complex

The BGU at Uitkomst comprises a phaneritic upper part and an aphanitic chill zone. The former is a highly variable rock (5 to 30% MgO, median 8.5%) and is described in detail by Gauert (1998). It has a variable texture, ranging from fine- to coarse-grained taxitic to equigranular, with major clinopyroxene (~20 to 30 modal %; $Wo_{34-49}En_{41-31}Fs_{25-20}$), orthopyroxene (<10 modal %; $Wo_4En_{64}Fs_{32}$), plagioclase (An_{30-55}; <50 modal %) and amphibole, and minor biotite, magnetite (-ilmenite), micropegmatite and quartz as primary magmatic minerals. The amphibole is edenitic and pargasitic with greenish rims of magnesio-hornblende and ferro-actinolite. Secondary phases include saussurite, clay minerals, chlorite, calcite, serpentine, talc, leucoxene and rutile.

The chill zone of the BGU (Agranier, 2000) is microcrystalline with clinopyroxene (~5 modal %; $Wo_{40}En_{36}Fs_{24}Ac_1$), orthopyroxene (~10 modal %; $Wo_3En_{53}Fs_{44}$), altered plagioclase (~20 to 40 modal %), hornblende (~20 to 60 modal %), biotite (<20 modal %) and ilmenite (~5 to 10 modal %) as major igneous minerals. Saussuritized plagioclase forms stubby plates (<0.5 mm in longest dimension) whereas the equant pyribole grains are ~0.2 mm in diameter. Hornblende replaces the other minerals. Secondary minerals include saussurite, chlorite, sphene, epidote and carbonate.

Lindeques Drift Intrusion

The Lindeques Drift intrusion is dominated by even-grained speckled and porphyritic spessartite (De Waal *et al.*, 2005; Bisschoff, 1972). Euhedral to anhedral phenocrysts (<20 mm in diameter) of amphibole (up to 50 modal %), comprising brown edenite and hastingsite with narrow green rims of magnesio-hastingsite and magnesio-hornblende, are set in a fine- to medium-grained matrix of salitic to augitic clinopyroxene ($Wo_{45.4}En_{33.7}Fs_{17.8}Ac_{3.1}$ to $Wo_{42.1}En_{40.6}Fs_{15.7}Ac_{1.6}$) (20 to 80 modal %), amphibole, plagioclase ($An_{12.1 \pm 12.7}$) (usually <25 modal %), biotite, magnetite(-ilmenite) (<25 modal %), micropegmatite and apatite.

Clinopyroxene, magnetite(-ilmenite) and apatite, all forming sub- to euhedral crystals, are cumulus phases. The amphibole is late magmatic, replacing clinopyroxene, magnetite(-ilmenite) and plagioclase (?) and has a reaction relationship with these minerals. The paragenetic sequence is magnetite(-ilmenite)-clinopyroxene-apatite-amphibole/plagioclase-sphene-biotite. Plagioclase and amphibole crystallization probably overlapped to some extent. Alteration roducts include chlorite, epidote, saussurite and sphene.

The Lindeques Drift intrusion contains small amounts of gabbroid rocks (De Waal *et al* 2005; Bisschoff, 1972). These occur as crosscutting dykes and sills and typically include diorite (alkali feldspar-greenish brown hornblende-augite-magnetite-apatite-sphene-quartz), leucodiorite (albite>>hornblende-augite-magnetite-apatite-sphene-quartz), syenodiorite (K-rich diorite commonly with alkali feldspar as a cumulus phase) and coarse-grained pegmatite schlieren (albite-brownish green hornblende-microperthite).

Bisshoff (1972) noticed that on the farm Boschdraai the spessartite apparently crystallized from the walls of the intrusion inward. Pegmatite schlieren in the spessartite increase towards the syenodiorite core of the intrusion, which lacks schlieren. The pegmatite schlieren seem to represent remnants of interstitial liquid transferred from the early spessartite mush towards the central part of the intrusion.

Heidelberg Intrusion

The Heidelberg Intrusion is composed of spessartite, petrographically comparable to the Lindeques Drift Intrusion (De Waal *et al.*, 2005). However, modal analysis indicates larger quantities of amphibole in the former relative to the latter.

Roodekraal Complex

Bisshoff (1972) and Clark (1972) described the lavas (MgO <5%) of the Roodekraal Volcanic Complex as amygdaloidal to massive, porphyritic to non-porphyritic andesite. Recent work (De Waal *et al* 2005) shows that the Roodekraal lavas are distinctly sodium-rich (Na_2O-2>K_2O), placing them in the hawaiite-mugearite-benmoreite series rather than in the andesite field. The porphyritic rocks display phenocrysts of tabular plagioclase (<An_{34}; <5 mm in long dimension) in a plagioclase-clinopyroxene-amphibole-magnetite (-ilmenite)-biotite-apatite matrix. The clinopyroxene is augite ($Wo_{39.5}En_{40.2}Fs_{18.3}Ac_{2.1}$) and the amphibole is dominantly ferrorichterite and ferrowinchite (De Waal *et al.*, 2005). Alteration products include sphene, chlorite, actinolite, sericite, calcite, magnetite, epidote-clinozoisite and minor quartz. Subordinate volcanic breccias (Clark, 1972) are associated with the lava and secondary hematite coatings are common in these rocks.

Diorite (MgO >5%) associated with the Roodekraal Complex (De Waal *et al.*, 2005; Bisshoff, 1972; Clark, 1972) consists of magmatic plagioclase (67 to 71 modal %; zoned, $An_{13.3 \pm 12.8}$), clinopyroxene (10 modal %), magnetite(-ilmenite) (7 to 19 modal %), biotite (<2 modal %), apatite (0.6 to 2.3 modal %), K-feldspar and olivine (traces). Late-magmatic amphibole (magnesio-hornblende, 4 to 9 modal %) pseudomorphously replaces augite ($Wo_{41}En_{37}Fs_{19}Ac_2$) (De Waal *et al.*, 2005). Secondary minerals include sphene, chlorite, stilpnomelane, sericite, calcite, magnetite, epidote-clinozoisite and minor quartz.

Clark (1972) described a 30 m thick differentiated sequence of modally layered diorite (An_{41}) that underlies a pyroxene andesite. The diorite contains magmatic magnetite(-ilmenite) (<40 modal %, concentrated in the basal part of the layer), clinopyroxene (<80 modal %; concentrated in the lower and middle part of the layer), plagioclase (An_{41}; <45 modal %), orthopyroxene (En_{81}; <40 modal %) and olivine (Fo_{81}; <10 modal %) (the latter three minerals concentrated towards the top of the layer). Amphibole is late magmatic and replaces the pyroxenes to a variable extent. Diorite aplite and pegmatite are subordinate.

Rietfontein Complex

The ultramafic to mafic rocks of the Rietfontein Complex comprise two distinct series *i.e.* olivine diorite-wehrlite and subordinate troctolite-olivine diorite (Bisschoff, 1969; 1999).

Plagioclase (An_{57}), olivine ($Fo_{75\text{-}77}$), clinopyroxene ($Wo_{39}En_{39}Fs_{22}$-$Wo_{39}En_{41}Fs_{20}$), orthopyroxene (En_{81}), amphibole and magnetite(-ilmenite) are the major phases in the olivine diorite-wehrlite. Olivine and clinopyroxene appear to be cumulus phases and amphibole is late magmatic. With plagioclase content decreasing from ~45 to ~5 modal %, the clinopyroxene content increases from ~35 to ~65 modal %. Over the same interval, olivine, magnetite(-ilmenite) and amphibole remain roughly constant at 22, 4 and 1 modal %, respectively. Large oikocrysts of orthopyroxene are sporadically present in some of the wehrlite samples (<7 %) (Bisschoff, 1969).

The troctolite (Bisschoff, 1969) contains small crystals of olivine (Fo_{77}) and plagioclase (An_{57}) enclosed in larger poikilitic clinopyroxene hosts. Magnetite and amphibole form minor phases. The rock displays igneous lamination due to the parallel orientation of the plagioclase laths. The troctolite grades into olivine diorite in which the poikilitic clinopyroxene ($Wo_{42}En_{38}Fs_{20}$) becomes granular and of a size comparable to that of the olivine. In the troctolite, with plagioclase decreasing from 50 to 25 modal %, olivine increases from 30 to 70 modal %, whereas clinopyroxene decreases from 10 to 2% and magnetite from 8 to 4%. In contrast, the olivine diorite shows little variation with olivine (41 ± 4 modal %), clinopyroxene (31 ± 5 modal %), plagioclase (20 ± 2 modal %), amphibole (8 ± 5 modal %) and magnetite (1 ± 0.2 modal %).

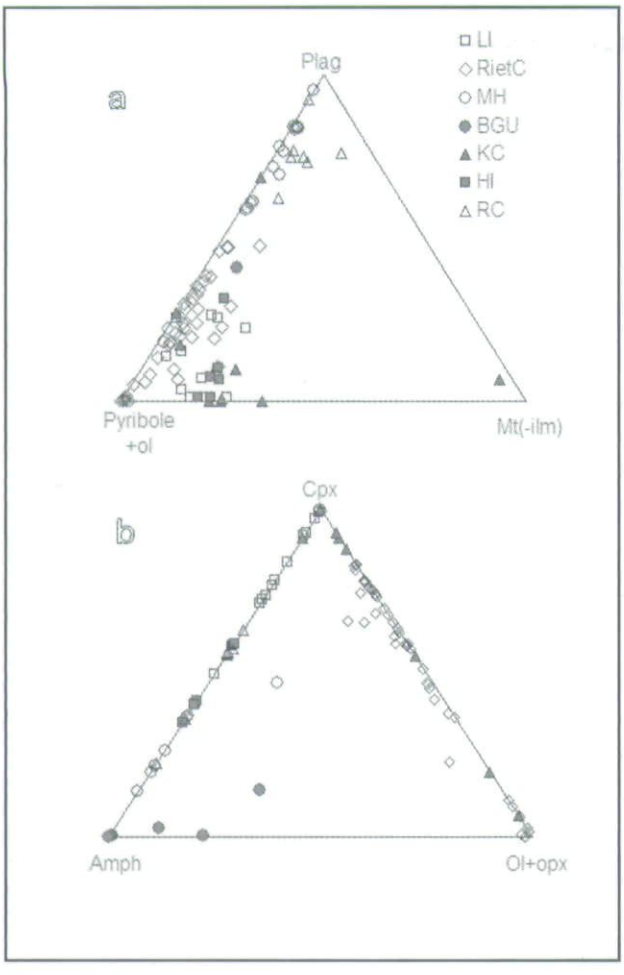

Figure 2. Modal data on the HITIS. (**a**) Mt(-ilm) is an important phase throughout, with increasing proportions in the cumulate rocks (base of triangle). For the Roodekraal lava, the mt(-ilm) values include sulphide. (**b**) The rocks from the Schoongezicht and Rietfontein Complexes are enriched in olivine and orthopyroxene with incipient amphibole development. Orthopyroxene is present in notable quantities in the Basal Gabbro Unit of the Uitkomst Complex. Legend the same as for (a).

Schoongezicht Complex

The Schoongezicht Complex (originally called the Kaffirskraal Complex, Frick, 1975, 1979) is dominated by a magnetite(-ilmenite) clinopyroxenite comprising clinopyroxene (average 69 modal %) and magnetite (-ilmenite) (average 24%) with minor biotite, amphibole and sulphide. Subordinate lenses of magnetite dunite (average 61 modal % olivine and 35 modal % magnetite-ilmenite), magnetite wehrlite (average 35 modal % olivine, 43 modal % clinopyroxene and 22 modal % magnetite-ilmenite), magnetite websterite (average 69 modal % clinopyroxene, 25 modal % magnetite-ilmenite and 6 modal % orthopyroxene) and magnetitite are interlayered with the magnetite clinopyroxenite. In these rocks, the clinopyroxene is an augite ($Wo_{41}En_{42}Fs_{15}Ac_2$), the orthopyroxene is $Wo_2En_{65}Fs_{33}$, and the olivine is $Fo_{70 \pm 5}$. The magnetite-ilmenite phase contains about 12% TiO_2.

The layered rocks may contain xenoliths, usually with sharp contacts, of gabbro and norite. More complex associations of feldspathic rocks, with discordant contacts and conspicuously low magnetite contents, are also developed in places (Frick, 1975; 1979). The latter associations comprise feldspathic clinopyroxenite, grading upwards into norite and finally gabbro. The feldspathic clinopyroxenite locally becomes pegmatitic and enriched in sulphide. In the feldspathic rocks, clinopyroxene is a salite ($Wo_{48.4}En_{33.2}Fs_{17.1}Ac_{1.3}$), and plagioclase is andesine ($An_{43 \pm 12}$).

Amphibole, replacing pyroxene, is a subordinate constituent in the Schoongezicht rocks (Frick, 1973; 1979) when compared with the spessartite (clinopyroxene-magnetite-ilmenite cumulate) of the Lindeques Drift and Heidelberg Intrusions (De Waal *et al.*, 2005).

High-Ti and FeTiP lavas

The high-Ti basalt and FeTiP lava (Schweitzer *et al.*, 1995) are porphyritic to glomeroporphyritic and in places amygdaloidal. The phenocrysts are plagioclase and clinopyroxene, variably replaced by amphibole and chlorite. The groundmass consists of decussate plagioclase laths ($An_{40;}$ <0.3 mm in length) with interstitial clinopyroxene, altered to actinolitic amphibole and chlorite, opaque minerals and sphene. Patches of devitrified glass are present in some samples.

Vredefort alkali granite

The Baviaankranz and Schurwedraai alkali granite (Elsenbroek, 1991, 1995) consist of quartz (26 to 49 modal %), albite (21 to 24 modal %) and K-feldspar (19 to 39 modal %) with subordinate (<10%) aegerine, arfvedsonite, Mg-lepidomelane, apatite, magnetite, epidote, zoisite and zircon. The quartz-albite-K-feldspar ratio varies considerably from one locality to the next. In the northeastern section of the Schurwedraai pluton the quartz content falls below 5%. In this area nepheline syenite xenoliths are common in the granite.

Summary of the petrography of the HITIS

It is evident from the foregoing section that the rocks of the HITIS have a relatively simple mineralogy. The alkali granite contains essentially magmatic alkali feldspar, quartz and Na-rich pyriboles, whereas six primary magmatic phases, *i.e.* clinopyroxene, FeTi-oxide (magnetite-ilmenite), amphibole, olivine, orthopyroxene and plagioclase make up the bulk of the mafic rocks (Figure 2). Subordinate magmatic minerals are apatite, quartz, biotite, sphene, zircon, chalcopyrite, pyrrhotite, pyrite and K-feldspar, which together seldom exceed 10 modal % of the rocks. Secondary minerals include chlorite, epidote, calcite, saussurite, scapolite, grossularite, sericite and pyrite. Locally the primary magmatic minerals have been completely destroyed and replaced by two or more of the secondary phases.

Regardless of the locality and rock type, the clinopyroxene in the mafic rocks of the HITIS typically is a light green salite or augite (Figure 3). The amphibole is calcic with edinitic and hastingsitic varieties

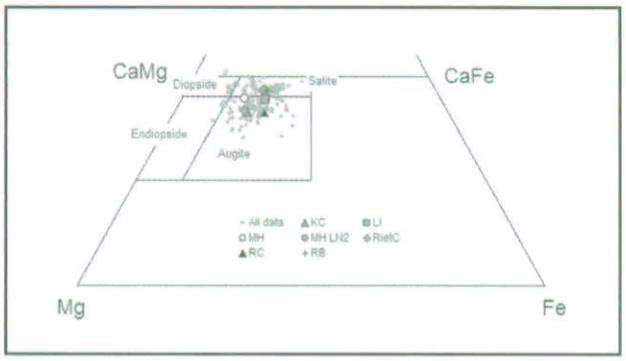

Figure 3. Compositional variation of clinopyroxene illustrated on the pyroxene quadrilateral. Bulk average compositions are shown for selected HITIS occurrences. Nomenclature after Le Bas (1962).

predominating (Figure 4). NaCa-amphibole (richterite and ferro-richterite) is prevalent in the Roodekraal volcanic rocks, whereas magnesio-hornblende, actinolite and ferro-actinolite, indicating late-stage re-equilibration, are common throughout the HITIS. Plagioclase, as a general rule, has anorthite contents of less than 50%. Exceptions are found only in the feldspathic xenoliths of the Schoongezicht Complex, the phaneritic portion of the BGU at Uitkomst and the metamorphosed melagabbronorite (X514) from Marble Hall. The magnetite contains lamellae as well as irregular segregations of ilmenite, the latter increasing in relative quantity in the chemically more evolved rocks.

Orthopyroxene, olivine and quartz are not common minerals in the mafic rocks of the HITIS but when present can become major constituents. Orthopyroxene reaches concentrations up to 6 modal % in some wehrlite samples of the Rietfontein Complex (Bisschoff, 1969), 13 modal % in melagabbronorite (X514) in the Marble Hall area, and up to 58 modal % in the feldspathic rocks of the Schoongezicht Complex.

Olivine is a major mineral in some of the ultramafic rocks of the Schoongezicht, Rietfontein and Koedoesfontein Complexes (Bisschoff, 1969; Frick, 1975; 1979). Clark (1972) described olivine from a cumulate rock (~8 modal % olivine) and lava (<5 modal % olivine) in the Roodekraal Complex. Traces of olivine are present in Marble Hall diorite and in the hybrid rocks of the LN2 body, whereas olivine is the dominant phase in the LN1 body.

Quartz is a scarce mineral in the more primitive mafic rocks of the HITIS, but it becomes a minor constituent (<5 modal %) in the more evolved dioritic rocks (Marble Hall, Roodekraal, Lindeques Drift). Locally, concentrations of up to 25 modal % were observed in the leucodiorite from Marble Hall (De Waal, 1963).

The different rock types representing the HITIS are summarized in Table 1.

Geochemistry

Major elements

A database, comprising a total of 265 whole rock chemical compositions of HITIS rocks, has been

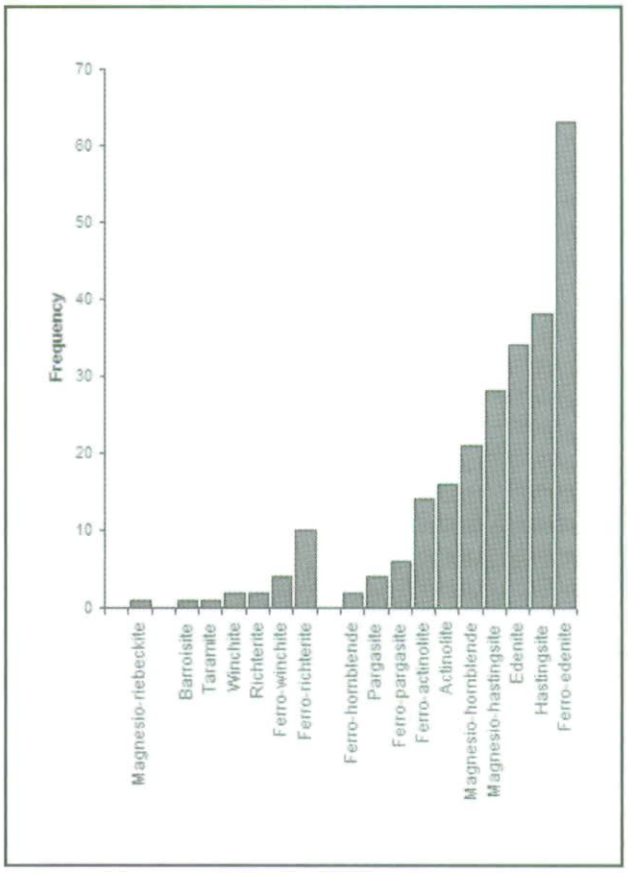

Figure 4. Frequency distribution of HITIS amphibole.

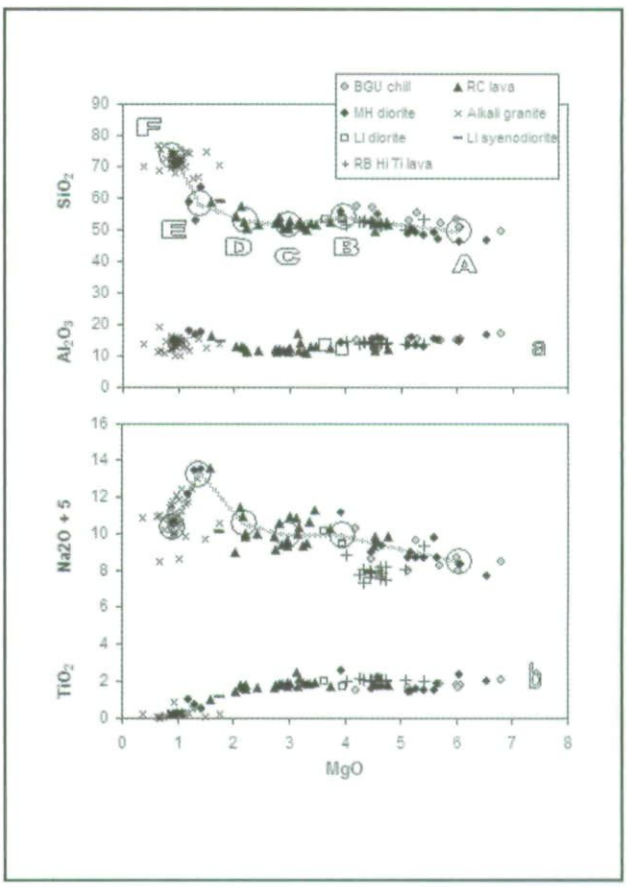

Figure 5. Liquid line of descent of the HITIS illustrated on a MgO-based binary diagram.

Table 1. Summary of main rock types of the HITIS

Rocktype	Essential petrography	Rock suite and reference
Alkali granite	Qz-albite-Kfsp rock with variable subordinate (<10%) aegerine, arfvedsonite, Mg-lepidomelane, apatite, magnetite, epidote, zoisite and zircon	Baviaankranz and Shurwedraai plutons[9], Rietfontein Complex[6], Heidelberg Intrusion[2] and Koedoesfontein Complex[6]
Diorite and meladiorite	Cpx-amphibole-plag rock with minor (<~10%) mt(-ilm), apatite, biotite and sphene. Post-emplacement fractionation rare and limited to local cpx and/or mt(-ilm) enrichmnent	Marble Hall sills1
	Fine-grained cpx-plag-amphibole-mt(-ilm) rock with apatite and sphene, and biotite phenocrysts	Lindeques Drift dykes and sills[2]
Feldspathic pyroxenite	Opx-cpx(-ol) cumulate with intercumulus plagioclase, magnetite(-ilmenite) and biotite; olivine and orthopyroxene has reactional relationship	Schoongezicht Complex[3]
Gabbro	Cpx(-opx-plag) cumulate with minor biotite, magnetite(-ilmenite), micropegmatite and quartz. Amphibiole replaces earlier pyribole. Taxitic texture in places.	Uitkomst Complex[11]
Gabbro, norite	Xenoliths	Schoongezicht Complex[3] Marble Hall sills[4]
Hybrid rock	Hybrid consisting of variably digested calc-silicate material in diorite	Marble Hall sills[4]
Leucodiorite to sodic anorthosite	Plag(-qz-Kfsp) aggregations associated with diorite	Marble Hall sills[1]
Mafic lava	Mugearite lava flows, plagioclase-phyric	Roodekraal Complex[2]
	High Ti basalt flows	Rooiberg Group[5]
	FeTiP lava flows	Rooiberg Group[5]
Magnetite clinopyroxenite and -websterite	Cpx-mt(-ilm) ± opx cumulate with minor (<2%) interstitial ol, plag, biot and spd	Schoongezicht Complex[3]
Magnetite dunite	Ol-mt(-ilm) cumulate with minor (<7%) interstitial cpx and spd	Schoongezicht Complex[3]
Magnetite wehrlite	Cpx-ol-mt(-ilm) cumulate with interstitial bio and spd; also mt(-ilm)-cpx cumulate with minor (<1%) interstitial ol, biot and spd	Schoongezicht Complex[3]
Magnetitite	Mt(-ilm) cumulate with interstitial ol, plag and spd	Schoongezicht Complex[3]
Melagabbronorite	Opx-cpx-plag rock (metamorphosed)	Dyke, Marble Hall Fragment[10]
Norite	Cpx-opx-plag-mt (micronorite) with flow texture in marginal zone	Schoongezicht Complex[3]
	Opx-plag-cpx as xenoliths	Schoongezicht Complex[3]
Olivine diorite	Mt(-ilm)-cpx –plag-olivine-amphibole rock with minor apatite and sphene.	Roodekraal Complex[8]
	Olivine-cpx -plag rock with minor (<~10%) mt(-ilm), amphibole and apatite.	Rietfontein Complex[6,7]
Spessartite	Mt(-ilm)-cpx cumulates with amphibole phenocrysts and interstitial plag, sphene, biot and apatite	Lindeques Drift Intrusion[2], Heidelberg Intrusion[2], Rietfontein Complex[6,7], Koedoesfontein Complex[6,7]
Syenodiorite	Fine-grained cpx-plag-amphibole-microperthite rock with apatite and sphene,	Lindeques Drift dykes and sills[2]
Troctolite	Ol-cumulates	Rietfontein Complex[6,7]
Wehrlite	Ol-cpx cumulates	Rietfontein Complex[6,7], Koedoesfontein Complex[6,7]

[1] De Waal and Armstrong, 2000
[2] De Waal *et al.*, 2005
[3] Frick, 1975, 1979
[4] Graham *et al.*, 2005
[5] Schweitzer *et al.*, 1995
[6] Bisschoff, 1969
[7] Bisschoff, 1999
[8] Clark, 1972
[9] Elsenbroek, 1991, 1993
[10] De Waal, 1963
[11] Gauert , 1998

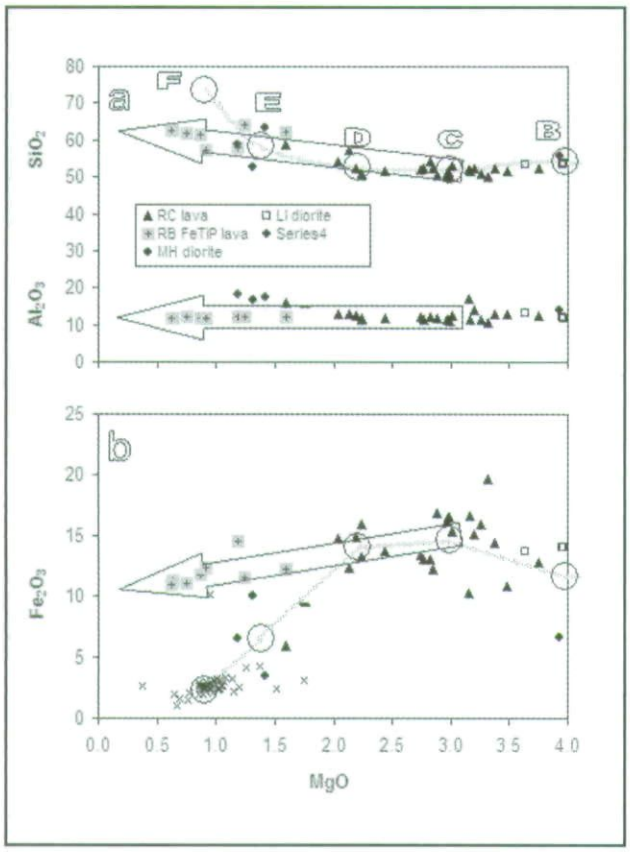

Figure 6. The FeTiP lava of the Rooiberg Group plots on an extension (arrows) of fractionation stage CD, suggesting a local deviation from the overall HITIS liquid trend.

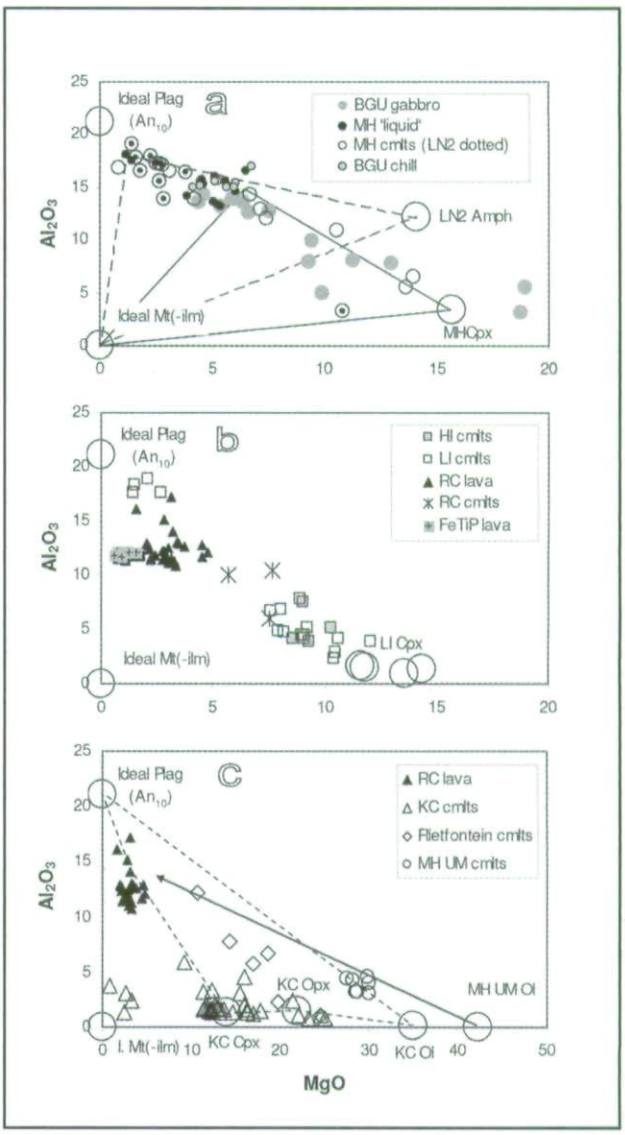

Figure 7. Cumulate rocks of the HITIS. (**a**) The MH and BGU cumulates plot within the mt(-ilm)-cpx-primitive MH liquid triangle (solid lines) largely along the cpx-liquid join. Two samples from the BGU (MgO ~18%) reflect opx/ol segregation. Amph and amph-plag segregations of the LN2 body at Marble Hall plot largely within the mt(-ilm)-amph-evolved diorite liquid triangle (stippled lines) with some overflow of the amph-plag cumulates towards plag. (**b**) The cumulates from the LI are represented by plag cumulates (MgO <3%) plotting roughly between the liquid (RC lava compositions) and plagioclase. The plag-cpx-mt(-ilm) cumulates (spessartite, MgO >7%) of the LI, HI and local cpx-mt(-ilm) segregations in the RC lava plot along the liquid-cpx join. (**c**) The ultramafic rocks from the Riet C, Schoongezicht (KC cmlts), and Koedoesfontein Complex are distributed between mt(-ilm) and cpx, opx and olivine. Feldspathic rocks in the RC projects up towards plagioclase.

compiled for the purpose of this study. These include the data on the Marble Hall sills and breccia (this study), chill zone and gabbroid rocks of the Basal Gabbro Unit of the Uitkomst Complex (this study; De Waal and Armstrong, 2000; Strauss, 1995; Gauert, 1998; Gauert *et al.*, 1995), the Lindeques Drift and Heidelberg Intrusions (this study; De Waal *et al* 2005; Bisschoff, 1969; 1972), the Rietfontein and Koedoesfontein Complexes (Bisschoff, 1969), the Schoongezicht Complex (Frick, 1975; 1979), the high-Ti basalt and high FeTiP lava of the Rooiberg Group (Schweitzer *et al.*, 1995), and the Vredefort alkali granite (this study, Graham *et al.*, 2005; Elsenbroek, 1993).

The chemical variation in the rocks regarded as HITIS liquids is illustrated in Figures 5a and b, which are based on 121 whole rock compositions. Inspection of the major elements suggests that the overall trend consists of five near-linear stages (Figure 5a) of development, starting at MgO ~6.5% (A) and ending at MgO ~0.5% (F), with inflection points at MgO values of approximately 4.5 (B), 3.0 (C), 2.2 (D) and 1.3 (E) %. Stage AB, the most primitive part of the liquid line of descent, is described by diorite from Marble Hall, the BGU chill zone rocks from Uitkomst, and the Rooiberg high-Ti lava. The mugearite lava and diorite from Roodekraal, diorite from Lindeques Drift, and the Rooiberg high-Ti lava support stage BC. Stages CD and DE are, less reliably, defined by Roodekraal lava and diorite, Lindeques Drift diorite and syenodiorite and Marble Hall diorite. The last stage, EF, is based on the chemical data of the Vredefort alkali granite. The estimated composition of the HITIS liquid at points A, B, C, D, E and F, derived by averaging compositional data straddling the inflection points, are shown in Figure 5a and listed in Table 2. It should be noted that the FeTiP lava (Schweitzer, 1998) do not follow the trend

depicted in Figure 5. Instead, these rocks scatter along a straight line extension of stage CD, as illustrated in Figure 6. The significance of this deviation will be discussed in due course.

The cumulate rocks associated with the Marble Hall sills are largely clinopyroxene (MgO >5%), amphibole or amphibole-plagioclase (MgO <5%) aggregates with highly variable interstitial magma contents. The amphibole and amphibole-plagioclase cumulates originating from the LN2 body (Graham *et al.*, 2004) seem to have had an evolved parent (MgO ~1.5%, Figure 7a). In contrast, the clinopyroxene cumulates, observed mostly in sills in boreholes south of Marble Hall, are apparently derived from more primitive diorite magma (MgO ~6%, Figure 7a). Variable aggregation of magnetite(-ilmenite) in all these cumulates are indicated in Figure 7a by the samples that plot towards the origin of the graph.

The phaneritic rocks of the BGU of the Uitkomst Complex (Gauert, 1998) are dominantly clinopyroxene-plagioclase cumulates (Figure 7a). Two samples (MgO ~18%) also contain notable quantities of orthopyroxene.

De Waal *et al.* (2005) recently showed that the spessartitic rocks of Lindeques Drift and Heidelberg

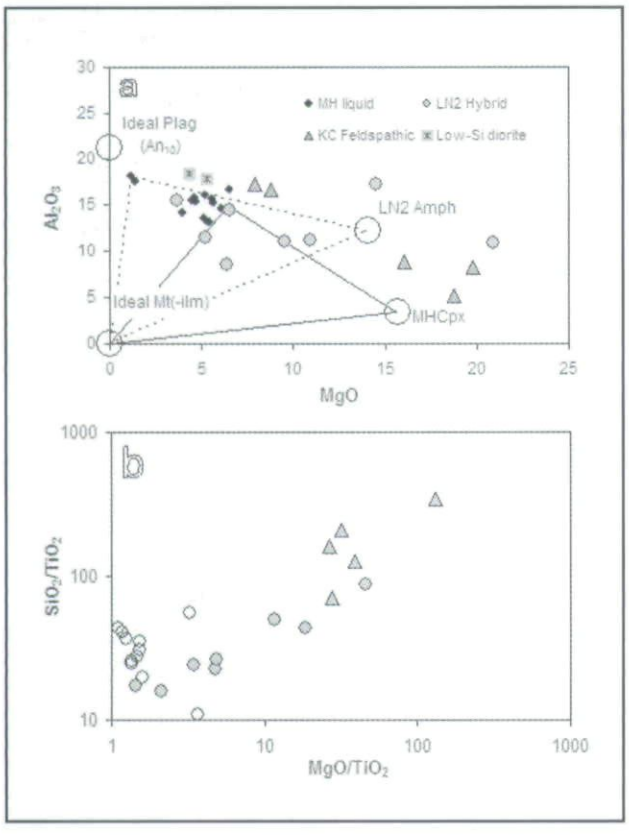

(Figure 8. Hybrid rocks: (**a**) The hybrid rocks of the MH LN2 body scatters away widely from the liquid composition towards high MgO values. Feldspathic rocks in the KC follow the same general trend. Low-Si diorite is from the LI (see text). (**b**) Ratio diagram distinguishes clearly between igneous cumulates (open circles) and hybrid rock in the MH LN2 body. The KC feldspathic rocks follow the same trend as the hybrid rocks giving a clue to their metasomatic origin.

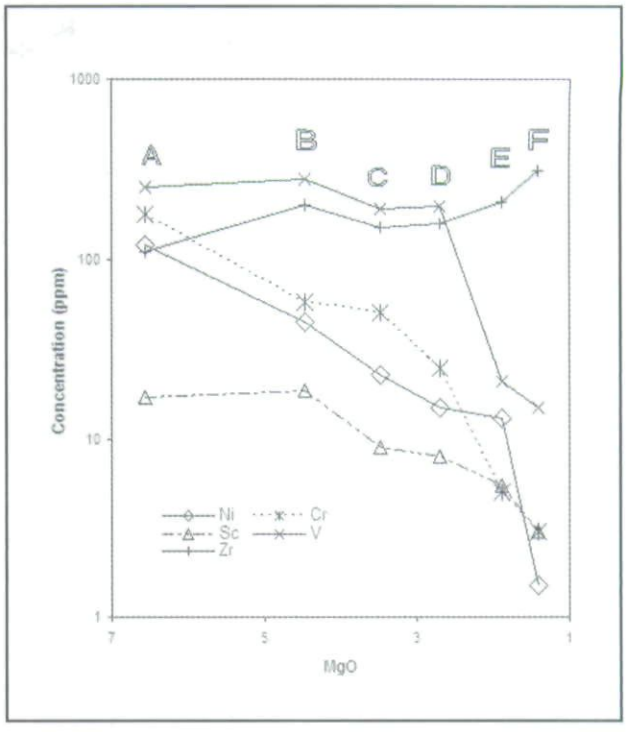

Figure 9. Trace element variations in the HITIS along the liquid line of descent. The nodes, A to E, correspond to those in Figure 5a. Minor discrepancy for V, Sc and Zr between nodes A and B may be due to regional variation in melt extraction conditions and fractionation detail.

Intrusions are essentially clinopyroxene-magnetite (-ilmenite) cumulates with low fractions of interstitial magma, a fact compatible with the distribution of these rocks in Figure 7b. Plagioclase segregation in the evolved syenodiorite (De Waal *et al.*, 2005) is reflected in the cumulates that plot at MgO ~2% (Figure 7b). Some of the Roodekraal lavas show enrichment in clinopyroxene (RC cmlts, Figure 7b) and some of the lavas (Al_2O_3 >~14%; Clark 1972) might reflect plagioclase accumulation.

The ultramafic rocks of the Schoongezicht Complex, described by Frick (1975; 1979), are dominantly clinopyroxene±magnetite(-ilmenite)±olivine±orthopyroxene cumulates which is in line with their distribution in Figure 7c. Since the composition of the parental magma of the Schoongezicht intrusion is unknown, the composition of the Roodekraal lava is shown Figure 7c for comparative purposes. The olivine±clinopyroxene and clinopyroxene± plagioclase±orthopyroxene cumulates of the Rietfontein and Koedoesfontein Complexes described by Bisschoff (1969) plot in the area demarcated by the stippled line in Figure 7c, which conform to their cumulate nature in from a Roodekraal-type magma. The olivine cumulates of the LN1 body at Marble Hall scatter between the Marble Hall liquid compositions (arrowhead) and that of the olivine (MH UM Ol) in the same figure.

The hybrid rocks of the LN2 body at Marble Hall show a large amount of variation but roughly follow a trend away from the liquid composition towards high

Table 2. Estimations of chemical compositions of HITIS liquid at selected inflection points

Node/Inflection point	A	B	C	D	E	F
Major %						
SiO_2	49.49	54.06	51.86	52.73	58.48	73.49
TiO_2	1.89	1.89	1.90	1.70	0.78	0.21
Al_2O_3	15.49	13.32	12.54	12.04	17.06	13.33
Fe_2O_3T	12.44	11.62	14.70	14.09	6.51	2.37
MnO	0.16	0.17	0.16	0.22	0.09	0.05
MgO	6.05	3.97	2.99	2.20	1.38	0.90
CaO	9.29	7.33	4.79	5.25	4.05	0.29
Na_2O	3.46	4.90	4.94	5.52	8.17	5.36
K_2O	1.07	1.05	1.90	1.41	0.64	3.92
P_2O_5	0.15	0.31	0.49	0.62	0.36	0.01
Cr_2O_3	0.02	0.01			0.01	
CO_2	0.11	0.39	2.99	4.93	0.51	
H_2O+	1.06	0.84	1.23	0.99	0.96	
H_2O-		0.00	0.18	0.28		
S	0.76	0.04			1.34	
Sum	101.43	99.91	100.67	101.95	100.33	99.94
Mg#	0.57	0.50	0.38	0.32	0.42	0.61
Trace ppm (XRF)						
Ni	121	45	23	15	13	2
Cu	97	112	357	361	119	9
Zn	72	81	101	136	27	26
Ga	18	24	23	13	24	16
Rb	35	27	55	54	19	73
Sr	399	378	451	336	463	131
Y	22	28	19	17	29	14
Zr	112	200	151	159	208	310
Nb	11	13	17	22	16	20
U	4	4			3	2
Th	2	6			5	9
Pb	5	4	6	12	11	8
Co	78	60	69	78	50	31
Cr	181	58	51	25	5	3
V	252	279	192	200	21	15
Ba	111	199			451	0
Sc	17	19	9	8	6	3
S			122	156		174

Trace ppm (ICP-MS)	A	B	C	D	E	F
La	19.2	22.4	27.2	32.7		17.2
Ce	43.2	45.9	52.1	60.6		30.3
Pr	5.7	5.6	6.0	6.6		2.4
Nd	24.0	22.5	23.1	24.0		7.0
Sm	5.4	4.6	4.1	4.0		1.0
Eu	1.8	1.4	1.2	1.1		0.2
Gd	5.2	4.3	3.7	3.4		0.7
Tb	0.8	0.6	0.5	0.5		0.1
Dy	4.5	3.8	3.1	2.9		0.9
Ho	0.9	0.7	0.6	0.6		0.2
Er	2.3	2.0	1.7	1.6		0.7
Tm	0.3	0.2	0.2	0.2		0.1
Yb	2.0	1.9	1.5	1.4		0.9
Lu	0.3	0.3	0.2	0.2		0.1
Hf	3.9	2.1	3.3	4.0		6.3
Ta	0.8	0.9	1.3	1.6		1.5
Pb	4.1		6.1	8.7		7.1
Th	3.1		4.0	5.9		6.1
U	0.8		0.5	0.7		1.0
Sc	17.5		10.7	8.7		0.9
V	139.0		205.0	203.0		10.1
Cr	25.8		24.2	3.1		2.7
Co	63.1		50.0	50.4		44.8
Ni	163.1		17.3	9.9		1.5
Cu	139.6		385.0	396.0		10.4
Rb	27.5		42.7	34.6		62.3
Sr	407.5		545.0	362.0		62.0
Y	22.7		16.2	14.7		5.1
Zr	175.5		126.1	149.0		270.0
Nb	12.7		22.1	25.0		21.5
Cs	1.1		1.8	2.2		0.5
Ba	201.8		504.0	388.0		389.0

CaO and MgO (Figure 8a) values. The feldspathic rocks of the Schoongezicht Complex (KC Feldspathic) follow this trend. Also shown on this diagram is the low-Si diorite found in the Lindeques Drift Intrusion, which De Waal *et al.* (2005) described as desilicated and de-aluminated ferrobasalt, due to reaction with carbonate rocks. A TiO_2-based ratio diagram (Figure 8b) clearly separates igneous cumulate rocks from hybrid rocks in the LN2 body at Marble Hall. The Schoongezicht feldspathic rocks also follow the hybrid trend indicating their xenolithic calc-silicate origin.

Trace elements

The database of whole rock compositions compiled in this study includes a number of older XRF analyses. Consequently the trace element dataset is not complete, and, moreover, biased towards the Marble Hall and Uitkomst rocks. However, it was still possible to make a reasonable estimation of the trace element concentrations at the six inflection points (Table 2) of the HITIS liquid line of descent.

As expected, the compatible elements (*e.g.* Ni and Cr) are exponentially depleted with decreasing MgO content (*i.e.* increasing degree of fractionation; Figure 9) whereas the incompatible elements (*e.g.* Zr) are exponentially enriched. Over the same interval, the concentrations of some elements (*e.g.* V, Sm and Sc) first increase and then decrease due to changing compatibility with the fractionating solid as the liquid evolves. On log-log binary diagrams, the trace element variation of stage AB (BGU chill zone and Marble Hall

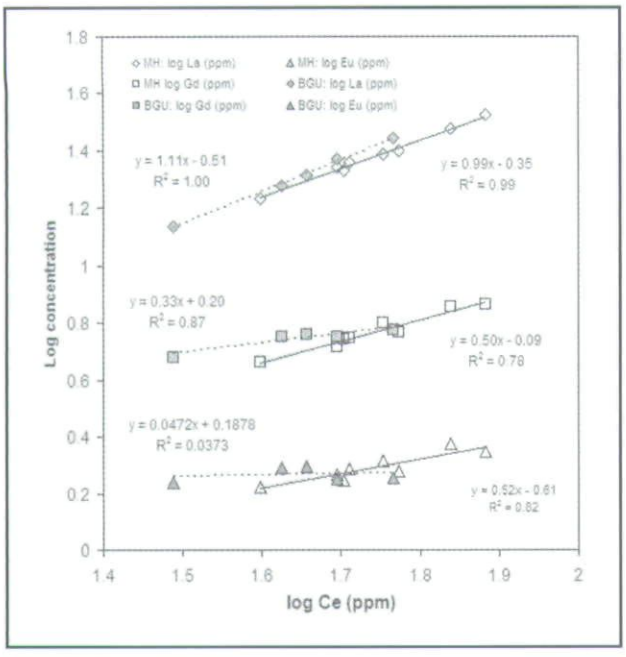

Figure 10. Trace elements in stage AB have linear relationships with high coefficients of determination, R^2. The linear regression equations are used to calculate partition coefficients for stage AB of the liquid line of descent (seen text for detail).

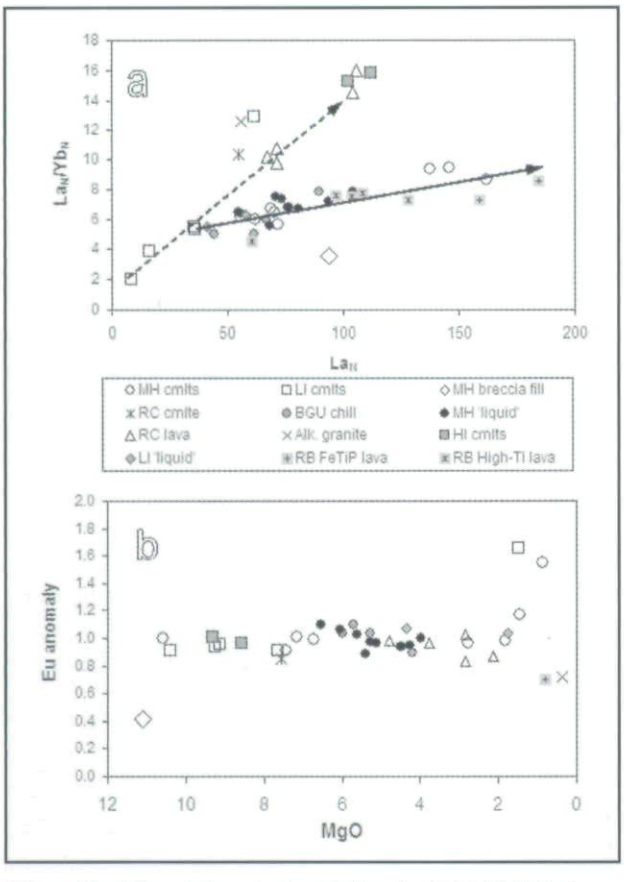

Figure 11. REE variations in the HITIS rocks. (**a**) LaN/YbN shows a difference in the degree of REE fractionation between the northern (MH, BGU, High-Ti and High FeTiP lavas) and southern (LI, HI, RC) magma systems. (**b**) Between 6.5 and 3% MgO, HITIS liquid does not display a distinct Eu anomaly. Below ~3% MgO, the deviations from unity become more pronounced in both the liquid and cumulate rocks.

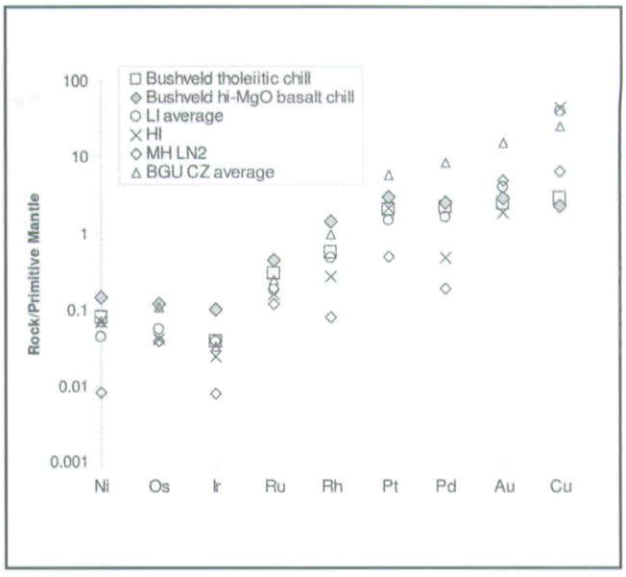

Figure 12. Normalized PGE patterns of selected HITIS rocks. The BGU chill zone is generally enriched in Rh, Pt, Pd and Au relative to the Bushveld tholeiitic chill zone and the other HITIS rocks. HITIS rocks show enrichment in Cu relative to the Bushveld chill rocks. Data for the Bushveld tholeiitic and high-MgO basalt chill zone (Wolfgang Maier, pers. comm., 2000) are given for comparison.

sills, Figure 5a) of the liquid line of descent show distinctly linear patterns (Figure 10), which suggest a homogeneous fractionating phase over the interval AB. Such data can be used to estimate the nature of the fractionating solid.

La_N/Yb_N in the HITIS liquid increases with increasing La_N. The HITIS rocks from the southern occurrences (LI, HI, RC in the Vredefort area; stippled arrow, Figure 11a) follow a steeper gradient than those from the northern areas (MH, BGU, High-Ti and High FeTiP lavas; solid arrow). However, some deviations from these trends exist. Two samples of the LI diorite (LI liquid, Figure 11a) appear to follow the shallower trend. An amphibole vein filling from the Marble Hall breccia has a markedly low La_N/Yb_N (~4) ratio, whereas the alkali granite and some Li and RC cumulates have relatively high values (La_N/Yb_N ~13 to 10 for Ln_N ~60).

Eu anomalies of the HITIS liquid roughly stay constant with decreasing MgO content in the range MgO between 6.5% and 3% (Figure 11b). Below 3% MgO, the Eu anomalies begin to deviate significantly from unity for both liquids (negative deviation) and cumulates (positive deviation). The Lindeques Drift, Heidelberg and Roodekraal cumulates with MgO >7% consistently have (Eu*-Eu) equal to or just below unity. The breccia fill has a markedly low ratio.

PGE data (Table 3, Figure 12) indicates a nickel-depleted and copper-enriched system. The HITIS PGE data shows a general correspondence to that of the tholeiitic magma series of the Bushveld Complex. However, the Uitkomst BGU chill zone rocks are visibly enriched in Rh, Pt, Pd, Au and Cu relative to the Bushveld tholeiitic chill. The other HITIS rocks are

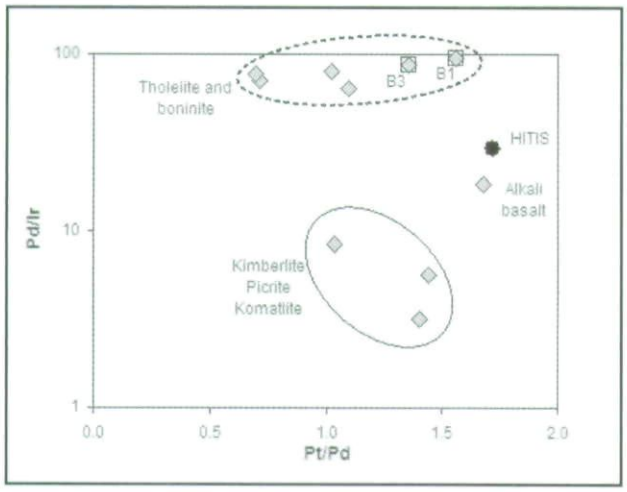

Figure 13. HITIS rocks plot close to alkali basalt on a ratio diagram of geometric means of mantle-derived magma types (data from Barnes and Maier, 2004).

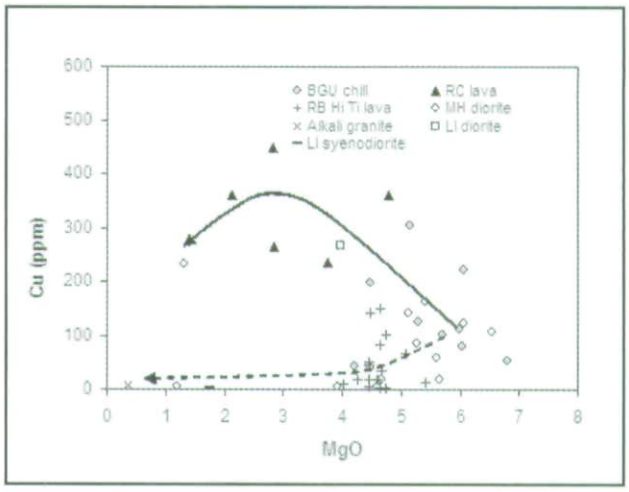

Figure 14. Cu concentration trends in the HITIS liquid line of descent show a high-Cu (solid arrow) and a low-Cu trajectory (stippled arrow).

depleted in all the precious metals except for Au and Cu when compared with the Bushveld tholeiitic chill

The Cu/Pd ratios are high and the Cu/Ni ratios appear to increase towards the more evolved HITIS rocks (Table 3). Using geometric means of the data for the different magma types listed in Maier and Barnes (2004), the HITIS rocks group with the alkali basalt (Figure 13).

Copper mineralization

Of the ten occurrences of HITIS rocks discussed in this paper, seven have notable copper sulphide mineralization associated with them. The Cu-contents of the evolving HITIS liquid follow either a high-copper trajectory (solid arrow, Figure 14) or a depleted path (stippled arrow). In the high-copper trajectory the metal reaches a maximum concentration (~400 ppm) at ~3% MgO, whereas for the depleted path the metal concentration remains below 25 ppm from 4 to 0% MgO.

The Marble Hall sills are generally depleted in copper and the samples representing liquids plot on the depleted path in Figure 14. The LN2 body is an exception in that it may contain up to 1% chalcopyrite in amphibole- and amphibole-plagioclase cumulates which are pervaded by late magmatic calcite-pyrrhotite-chalcopyrite veins (Graham *et al.*, 2004).

In the Uitkomst Complex, the Basal Gabbro Unit contains abundant disseminated sulphide, typically enriched in copper relative to the overlying lithological units (Van Zyl, 1996; Gauert, 1998; Hornsey, 1999; Maier *et al.*, 2004). The chill zone rocks, which are largely distributed along the high-copper trajectory in Figure 14, contain blebs of Cu-rich sulphide suggesting sulphide exsolution prior to emplacement. Chalcopyrite, locally op to 9 weight %, is associated with pentlandite and pyrrhotite in the clinopyroxene-plagioclase cumulates of the Basal Gabbro Unit (Hornsey, 1999; Gauert, 1998;

Table 3. PGE data on HITIS

Element	Conc. level	LI W1-67	LI W-79	LI OB1-111	HI P3-100	MH LN2-49	BGU* Phaneritic	BGU CZ* (S<0.15%)	Average
S	%	0.11	0.14	0.07	0.13	2.75	2.80	0.21	0.11
Ni	ppm	82	115	67	142	16	3562	139	91
Os	ppb	<0,42	<0,37	<0,33	<0,28	<0,26	17.65	0.37	0.21
Ir	ppb	0.114	0.238	0.044	0.083	0.027	35.452	0.110	0.116
Ru	ppb	<1.7	<2,0	<1,7	<1,6	<1,2	13	1.2	0.86
Rh	ppb	0.22	1.05	<0,15	0.26	<0,15	26.50	0.91	0.71
Pt	ppb	13	14	4	15	4	372.5	40	7
Pd	ppb	6.9	10.3	2.1	1.9	<1,5	462.5	32.8	4.3
Au	ppb	5.011	5.617	1.297	1.869	4.766	124.350	14.711	4.180
Cu	ppm	1168	1520	589	1227	177	6611.5	690	727
Re	ppb	0.07	0.12	0.16	0.22	0.22	9.82	0.80	0.45
Pd/Ir		60.3	43.4	47.9	23.0	28.0	13.0	298.8	37.4
Pt/Pd		1.8	1.4	2.0	7.8	4.7	0.8	1.2	1.7
Cu/Pd		169275	147573	280476	645789	236?	14295	21046	168477
Cu/Ni		14.2	13.2	8.8	8.6	11.1	1.9	5.0	8.0

*Average from Maier *et al.*, 2004

De Waal and Gauert, 1997; Van Zyl, 1996) where it forms a notable base metal sulphide deposit (Anon., 1997). The bulk average Cu/Ni ratio for BGU-associated disseminated sulphide ore body is 1.1, against values of less than 0.4 for the disseminated sulphide ore bodies in the overlying units (Anon., 1997). This is in line with earlier findings (De Waal and Armstrong, 2000; De Waal *et al.*, 2001) that the BGU is derived from a tholeiitic to alkali basaltic magma, whereas the overlying units of the Uitkomst Complex are products of a boninitic Bushveld B1-type magma.

Small Cu-rich sulphide bodies distributed mainly along fault and contact zones have been described from the Roodekraal Complex (Clark, 1972). High temperature magmatic chalcopyrite-pyrrhotite-pyrite segregations are hydrothermally overprinted, sequentially, by chalcopyrite-pyrrhotite-pyrite, chalcopyrite-chalcocite, and finally low temperature chalcocite-bornite.

Disseminated chalcopyrite, in concentrations of up to 1.5% and in association with pyrrhotite, is a common constituent of the spessartite of the Lindeques Drift and Heidelberg intrusions (De Waal *et al.*, 2005). Rocks from the Lindeques Drift Intrusion and the Roodekraal lava plot on the high-copper trajectory in Figure 14. De Waal *et al.* (2005) proposed that these two bodies are comagmatic.

The ultramafic cumulates of the Schoongezicht Complex are enriched in chalcopyrite and associated minor pyrrhotite and pyrite. Frick (1975; 1979) described average copper contents of 0.31% (~1 % chalcopyrite) in magnetite dunite and magnetite wehrlite, and 0.13% (~0.4% chalcopyrite) in magnetite clinopyroxenite and magnetite websterite. Combined precious metal contents of up to 0.6 g/t were observed in boreholes drilled in the Schoongezicht Complex (Frick, 1979).

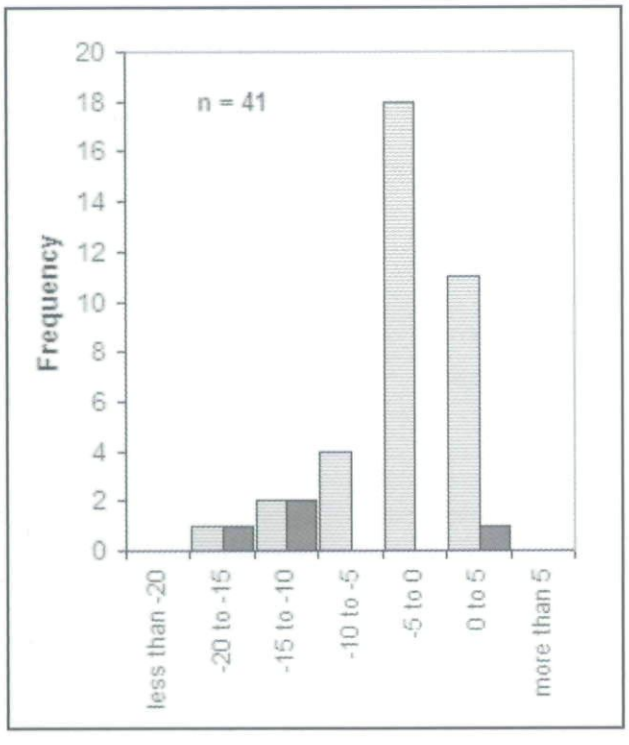

Figure 15. Sulphur isotopic ratios ($\delta^{34}S$) in the HITIS rocks peak between –5 and +2 permil (grey bars; median = – 0.18), but show a distinctive tail towards –20 permil. The latter is due to contamination of the Uitkomst BGU with metasedimentary rocks (black bars) that are generally depleted in heavy sulphur.

S isotopic ratios

The $\delta^{34}S$ values of 41 samples of HITIS rocks, illustrated in Figure 15, vary between minus 20 and 2 permil, with a distinct peak at about zero permil. The deviation towards negative $\delta^{34}S$ values in Figure 15 derives from samples of the BGU of the Uitkomst Complex, which was ascribed by Gauert *et al.* (1996) to local contamination by either Chuniespoort dolomite, or shale and quartzite belonging to the Pretoria Group. In general, these metasedimentary rocks appear to be depleted in $\delta^{34}S$.

Discussion

Calc-silicate xenoliths

The feldspathic xenoliths of the Schoongezicht intrusion have previously been considered as derived from deep-seated mafic sills (Rogers, 1922; Nel and Jansen, 1957) or representing early cognate cumulates (Frick, 1979) that are part of the igneous succession. We contend that all these feldspathic rocks are variably reworked carbonate/calc-silicate xenoliths in which the presence of pegmatite with associated enhanced sulphide concentrations and discordant layering all point to a xenolithic origin. Chemical signatures comparable to known hybrid/calc-silicate rocks (Figure 8) from Marble Hall support this interpretation.

The presence of carbonate/calc-silicate remnants in the Schoongezicht Complex indicates that this intrusion probably roofed in the Malmani dolomite, stratigraphically overlying the Ventersdorp Supergroup. The level of intrusion of the Schoongezicht Complex is therefore roughly comparable to that of the Rietfontein Complex further to the west.

Bushveld magmatic event

The ages listed in this paper for the Marble Hall sills (2056 ± 3 Ma) and breccia (2055.5 ± 3.1 Ma), the Uitkomst Complex (2044 ± 8 Ma), the Lindeques Drift Intrusion (2054.8 ± 5.7 Ma), the Roodekraal Complex (2053.9 ± 9.2 Ma) and the Vredefort alkali granite (2052 ± 14 Ma) are indistinguishable from that of the Bushveld magmatic event (*i.e.* Rustenburg Layered Suite: 2054.4 ± 2.8 Ma, R.A. Armstrong, personal communication; Lebowa Granite Suite: 2054 ± 2 Ma, Walraven and Hattingh, 1993; Rooiberg Group: 2061 ± 2 Ma, Walraven, 1997). In addition to these absolute ages, it is of note that the Marble Hall breccia contains xenoliths of Bushveld B1-type sill rock enclosed in a HITIS matrix (De Waal *et al.*, 2002), whereas at Uitkomst, the BGU precedes the overlying ultramafic units derived from the Bushveld B1-type magma (De Waal *et al.*, 2001). Since the Bushveld B1-type magma is regarded as parental to the Lower zone of the Bushveld Complex,

it may be inferred that the emplacement of the HITIS temporally overlapped the formation of the Lower Zone.

Co-lineage of undated HITIS bodies

Several intrusive and extrusive bodies (*i.e.* Heidelberg Intrusion, Rietfontein Complex, Schoongezicht Complex, Koedoesfontein Complex, high-Ti basalt and FeTiP lava) treated in this paper have not been dated by absolute methods. They are tentatively classified with the HITIS on the strength of their mineralogical, petrographic, petrologic (Table 1) and chemical (Figures 5, 6 and 7) characteristics (see also De Waal *et al.*, 2005 and Bisschoff, 1969, 1999 for more detail). However, whether or not this grouping is perfectly valid is not critical to the main thesis propounded in this paper. The need for further research is indicated.

The following aspects are regarded as important indicators of the kinship of the relevant bodies to the HITIS:

1. In general, all the undated bodies have high Ti contents as well as relative geological ages compatible with the dated bodies.
2. The association of alkali granite with ultramafic and mafic rocks of the HITIS, *i.e.* in the Rietfontein, Heidelberg and Koedoesfontein Complexes, supports the notion that the granite forms an integral part of the HITIS, and as suggested in this paper, probably represents the final phase in the liquid line of descent
3. The mineralogical, petrological and chemical similarities of the Heidelberg and Lindeques Drift Intrusions (De Waal *et al.*, 2005), as well as the presence of alkali granite veins in the former leave little doubt that these bodies are of the same age.
4. The ultramafic rocks of the Rietfontein Complex, containing cumulus sodic plagioclase, clinopyroxene and olivine (Bisschoff, 1969; 1999), are closely associated with alkali granite.
5. The dominant clinopyroxene-magnetite(-ilmenite) cumulates, the enrichment in chalcopyrite and the presence of calc-silicate xenoliths suggesting a contact with Malmani dolomite (see discussion on calc-silicate xenoliths) qualify the Schoongezicht Complex as a member of the HITIS.
6. The high-Ti basalt of the Rooiberg Group is chemically comparable to the HITIS rocks for all elements except Fe_2O_3T, CaO and Na_2O. For comparable MgO contents, the high-Ti basalt is depleted in Fe_2O_3T and CaO and enriched in Na_2O relative to the other HITIS rocks. One might provisionally invoke thermal metamorphic effects of the Bushveld Complex, or possible regional thermal variation in mantle melting regime, or local fractionation detail of the HITIS liquids. A more in depth investigation is clearly needed.
7. The FeTiP lavas of the Rooiberg Group are tentatively included in the HITIS. The mineralogy of these lavas is typical of HITIS rocks and their position on the MgO variation diagrams (Figure 6), together with their negative Eu anomaly (Figure 11b), suggest them to be plagioclase-depleted products of extended fractionation during stage CD.
8. The ultramafic Koedoesfontein rocks petrographically resemble those in the Rietfontein Complex and Lindeques Drift Intrusion and has alkali granite associated with them.

Differentiation

The change in the slope of the liquid line of descent relative to MgO, illustrated in Figure 5, requires a related compositional change in the fractionation products at each of the indicated nodes, A, B, C etc. The dominant mineralogical composition of the fractionating phases for each stage of the liquid line was derived, applying a addition-subtraction algorithm (see Methods of Investigation) followed by least squares optimization

Table 4. Tentative fractionation model for the HITIS

Stage	Mineralogy (estimated percentage in fractionating solid)	Conserved component	Estimated % solids crystallized	Critica evidence
AB	Amph (100) (±cpx±plag)	P_2O_5	53	Si enrichment excludes simple cpx-plag mixtures; high-Al phase required; amphibole fractionation is compatible with trace element distribution; Figure 16.
BC	Plag(58) Cpx(42)**	P_2O_5	17	Strong Fe enrichment; strong Sc depletion sets in; Ca and Si depletion increases.
CD	Plag(62) Cpx(21) Mt(-ilm) (17)**	P_2O_5	6	Fe and Ti depletion sets in; Si increases, Figure 6
DE	Cpx(70) Mt(-ilm)(30) * (+Ap±Ol±Opx)	Al_2O_3	7	Continued Fe and Ti depletion; strong P depletion sets in; strong V depletion sets in; Na enrichment. Fractionation products represented by the ultramafic cumulates from LI, HI, KC and RietC.
EF	Plag(72) Cpx(11) Mt(-ilm)(8) ** (+Ap)	K_2O	14	Enrichment in Rb; further Ti and P depletion; strong Ca and Al depletion. Residual melt of 3 weight % represented by the Vredefort alkali granite

** Estimated by addition-subtraction method followed by least squares optimization using selected end member compositions

*From De Waal *et al.* (2005)

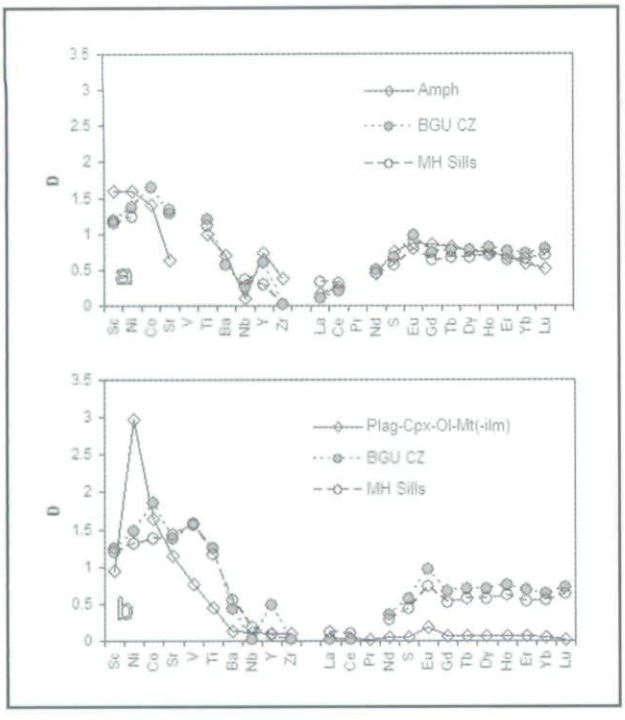

Figure 16. Comparison of published and observed partition coefficients, D, for the two fractionation models of stage AB. (**a**) Published data (Bedard, 1994) for amphibole (amph) closely mimic those observed for the BGU chill zone and Marble Hall sills. (**b**). The alternative model of plag-cpx-ol-mt-ilm fractionation is not supported by the observed data.a.

with selected compositions of olivine, clinopyroxene, plagioclase, magnetite and ilmenite in HITIS rocks as possible mineral phases. The estimated percentage of solids that crystallized in each fractionation stage is calculated from the increase in concentration of the conserved component for the given stage. The results, seen as reasonable estimates, are listed in Table 4.

The close correspondence between published D-values for amphibole (Bedard, 1994) and those calculated for differentiation stage AB (Figure 16a) supports the notion that amphibole fractionation dominated during this stage. Moreover, the major element composition of the fractionating solids for stage AB (not shown here) approaches that of pargasitic amphibole. It is suggested that intermittent tappings from a magma chamber fractionating mainly amphibole supplied the magma that intruded as sills at Marble Hall and at Uitkomst (BGU rocks). Although the data corresponds well with almost pure amphibole as the crystallizing phase in stage AB, co-precipitation of minor clinopyroxene and/or plagioclase can not be excluded. The resolution of the method precludes a definitive answer on this. However, an alternative model (*i.e.* olivine-clinopyroxene-plagioclase-magnetite-ilmenite) gives inferior results in terms of trace elements (Figure 16b).

The fractionation models for the following two stages (BC and CD) are tentative and based solely on major element estimation derived by the addition-subtraction method. Unfortunately, the available trace element database is not sufficient to test the validity of these major element models. Furthermore, we suspect that these two fractionation stages represent deep-level processes in the crust and that their fractionation products are not exposed at the current levels of erosion. The possibility that stage BC is an extension of stage AB, but with enhanced plagioclase fractionation can not be excluded.

The mineral composition of the fractionating solids proposed for stage DE is based on the findings of De Waal *et al.* (2005) on the Lindeques Drift and Heidelberg Intrusions and the Roodekraal Complex. It can also be shown, using the K_d(ol/melt); FeO/MgO) = 0.3 (after Roeder and Emslie, 1970), that the magma that was in equilibrium with the olivine found in the Rietfontein and Schoongezicht Complexes had an Mg# = 0.29 to 0.32, which approximates the Mg# of the HITIS liquid at node D (Table 2). The ultramafic cumulates found in these two bodies are interpreted to represent early crystal fractionates from a ferrobasaltic magma comparable to that which gave rise to the Lindeques Drift and Heidelberg Intrusions and the Roodekraal Complex (De Waal *et al.*, 2005).

The last stage, EF, is largely defined by the transition from highly evolved diorite to the Vredefort alkali granite. Predominantly plagioclase fractionation is indicated by the addition-subtraction-least squares method, which is compatible with the prominent negative Eu anomalies of the alkali granite. The latter is interpreted as the final liquid fraction, estimated to represent about 3 per cent of the initial liquid of the HITIS magma at node A. The observed scatter in the data (Figure 5) may be due to local differentiation and/or contamination with country rock as recorded by Elsenbroek (1991; 1993).

Finally, it is also possible to show that the olivine (Fo_{80}) in the ultramafic cumulates of the LN1 body at Marble Hall was in equilibrium with a magma with Mg# = 0.55 (based on calculation using the data of Roeder and Emslie, 1970). This suggests that this ultramafic cumulate may have formed from a primitive HITIS magma, close to node A (Table 2).

Parental magmas

The most primitive Bu magma observed until now has MgO contents of between 6.0 and 6.8%. Of the five samples in the database that have MgO >6%, only one is nepheline normative. However, published trace element discrimination diagrams ($Zr*P_2O_5*10^4$ vs. Nb/Y, Floyd and Winchester, 1975; $Zr*P_2O_5*10^4$ vs. TiO_2, Winchester and Floyd, 1976; TiO2 vs. Y/Nb, Floyd and Winchester, 1975; V vs. Ti, Shervais, 1982; Zr/TiO_2 vs.Y, Floyd and Winchester, 1975; and Zr/Y vs. Zr, Pearce and Norry, 1979), as well as the PGE data (Figure 13) given earlier, suggest these liquids to be 'within plate' and straddling the boundary of alkali and tholeiitic basalt. In addition, these primitive HITIS liquids are comparable in composition to transitional basalts from other parts of

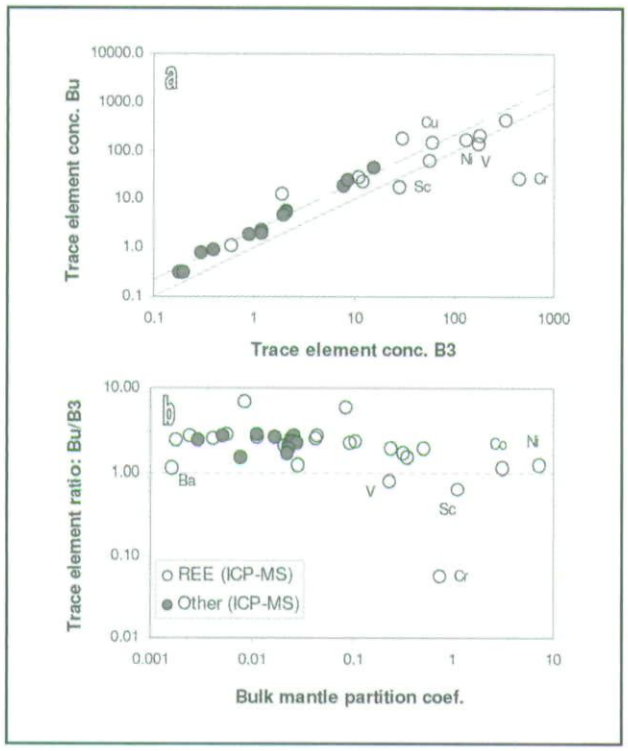

Figure 17. Incompatible trace elements are enriched in Bu magma relative to the B3 magma. (**a**) The REE show an enrichment factor of about 2.2 (stippled line), whereas the mantle-compatible elements show no significant enrichment. (**b**) The decrease in the Bu/B3 trace element ratio appears to be related to the garnet lherzolite-mantle bulk partition coefficient. Cr and Ba seemingly deviate significantly from the general trend.

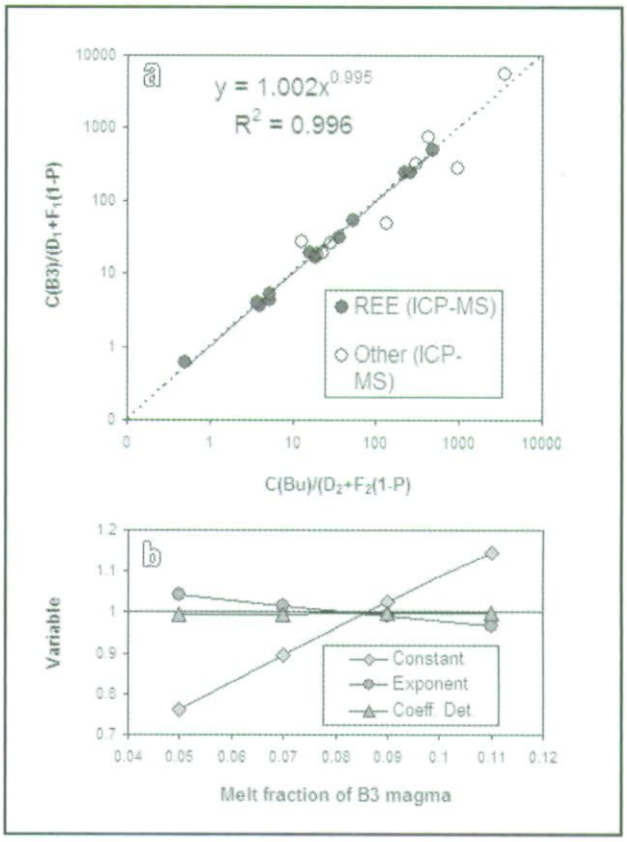

Figure 18. Garnet lherzolite melting model for the Bu and Bushveld B3-type magmas. (**a**) Least squares fit for Bu and B3 magma representing, respectively, 3.1 and 8.7% melt fractions. (**b**) Variation of the constant and exponent of the best fit equation, as well as the coefficient of determination, for varying assumed values for the melt fraction, F, of the B3-type magma. A unique solution is obtained at F = 8.7%.

the world, *e.g.* the Iblean volcanics (Beccaluva *et al.*, 1998).

The major element chemistry of the primitive Bu magma (node A, Table 2) shows the latter to be enriched in Ti, Fe, Na and K and depleted in Ca and Mg relative the Bushveld B3-type magma (Curl, 2001; Harmer and Sharpe, 1985). In terms of trace elements, the Bu magma is generally enriched in mantle incompatible elements relative to B3 (Figure 17). This raises the possibility that the Bu magma is the low fraction melt equivalent of the B3 magma. Assuming a batch melting process, it can be shown that

$$C_1/[D+F_2(1-P_2)] = C_2/[D+F_1(1-P_1)]$$

where C_1 and C_2 are the concentrations of a trace element after fractions F_1 and F_2, respectively, of the source have melted, and D and P are the bulk partition coefficients for the source mineralogy and the minerals in the melt fraction, respectively (Rollinson, 1993). Plotting $C_1/[D+F_2(1-P_2)]$ against $C_2/[D+F_1(1-P_1)]$

for two sets of trace element data presumed to represent different melt fractions from the same source, should then result in a straight line (y = x) with a slope of 1 and a c-intercept of 0.

This approach was applied to two different mineralogical compositions as mantle source (*i.e.* average garnet lherzolite comprising 63, 28, 4 and 5% olivine, orthopyroxene, clinopyroxene and garnet, respectively, and an average spinel lherzolite with 80, 10, 8 and 2% olivine, orthopyroxene, clinopyroxene and garnet, respectively; Maaloe and Aoki, 1977), using published partition coefficients (listings by Rollinson, 1993 and Bedard, 1994) and assuming the four respective minerals in each source composition melted in equal weight proportions (= modal melting). The results for 21 trace elements are illustrated in Figures 18 and 19.

Although both models had unique solutions, the garnet lherzolite model is internally more consistent than the spinel lherzolite model (compare error triangles in Figures 18b and 19b). The garnet lherzolite model suggests that the Bu magma could represent a 3% melt of a mantle source that yielded the Bushveld B3-type magma at 9% melting. The spinel lherzolite model in turn suggests the Bu and B3 to be 1 and 4% melts from a similar source, respectively. Unfortunately, the method does not allow any further discrimination between the two models. On the one hand the garnet lehrzolite model seems to be superior in terms of "goodness of fit", and on the other hand spinel lehrzolite, which typically contain amphibole and other hydrous phases (Maloee and Aoki, 1977), may better explain the wet nature of

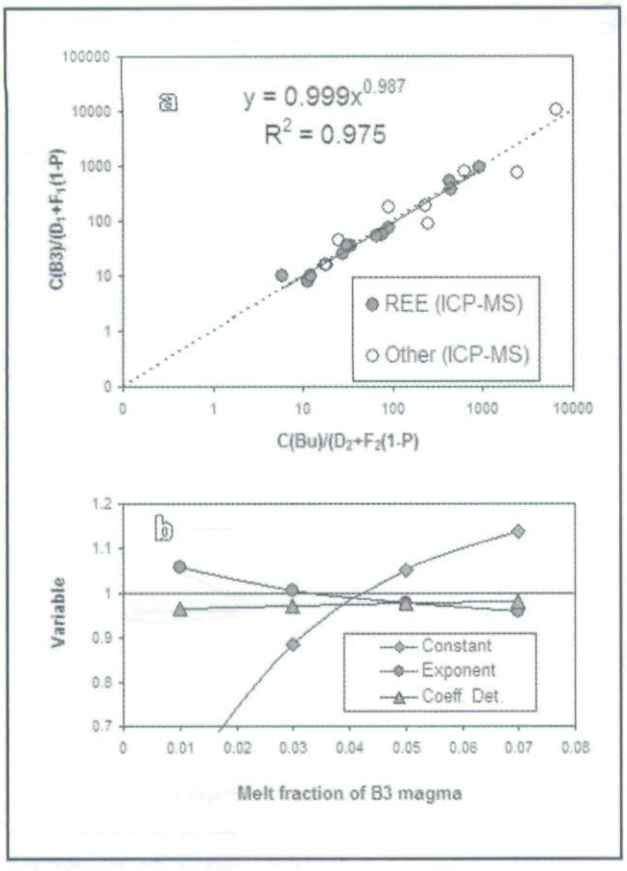

Figure 19. Spinel lherzolite melting model for the Bu and Bushveld B3-type magmas. (**a**) Least squares fit for Bu and B3-type magma representing, respectively, 1.2 and 4.2% melt fractions. (**b**) Variation of the constant and exponent of the best fit equation, as well as the coefficient of determination, for varying assumed values for the melt fraction, F, of the B3 magma. A unique solution is obtained at F ~4 to 5%. Note the enlarged error triangle between these values relative to that in Figure 18.

the HITIS magma. Whatever the final choice, the results of the modelling suggest that the Bu can indeed be a small fraction melt of a mantle source that ultimately yielded the tholeiitic B3-type magma.

Finally, it is also evident from the data presented in this paper that differentiation of the initial Mg-rich transitional basalt liquid yielded the ferrobasalt that is parental to the Lindeques Drift and Heidelberg Intrusions and the Roodekraal Complex (De Waal *et al.*, 2005) and, ultimately, the Vredefort alkali granite. Also, on average, it appears that the transitional basalt magma that produced the northern bodies (Marble Hall, Rooiberg, Uitkomst) had initial concentrations of incompatible elements slightly different from that of the basalt magma that fed the magmatic systems towards the south. This effect is seen for example in the trace element diagram (Figure 9) where Zr decreases instead of increases between nodes A and B. Such variance may be attributed to regional variation and, tentatively, a degree of lateral zoning away from the Bushveld "hot spot" centre.

A comprehensive model is proposed in Figure 20, which is an updated version of the model put forward by De Waal *et al.* (2005) for the HITIS rocks in the Vredefort area.

Water content

The HITIS rocks typically contain late magmatic amphibole, suggestive of water contents high enough to stabilize this mineral during the end-stages of crystallization of the magma. However, in the case of the Schoongezicht, Rietfontein and Koedoesfontein Complexes, amphibole formation is notably subdued. This raises the possibility of variable water contents in the parental magmas responsible for the individual bodies, and, in addition, that the hydration of the magmas could have been a shallow level localized phenomenon.

The answer to this question is most probably found in the amphibole-dominant fractionation process (shown earlier) during stage AB, and the fact that the same magma had olivine-clinopyroxene as the main ferromagnesian mineral on the liquidus in the Marble Hall sills and BGU chill zone. Experimental work by Green (1982) illustrated that amphibole-clinopyroxene is stabilized in wet tholeiitic magma crystallizing at high pressure (>*ca.* 5 kilobar), but at low pressure the same melt will have olivine-clinopyroxene on liquidus. We infer from this analogy that the primitive HITIS liquid inherited a relatively high water content on formation (low fraction melt of a metasomatized? mantle?) and crystallized amphibole at deep crustal levels (>ca. 15 km depth). However, on emplacement at the upper crustal levels, at Marble Hall and at Uitkomst, it reverted back to olivine-clinopyroxene crystallization. Accordingly, we propose that in the instance of Schoongezicht and Rietfontein, mentioned above, only the lower portions of the intrusions, that crystallized prior to amphibole stabilization, are exposed.

Cu mineralization

The high Cu/Pd and Cu/Ni ratios (average for low S samples; Table 3) of the HITIS rocks could suggest a magmatic system that already purged its sulphide charge before emplacement (as suggested for the BGU by Maier *et al.*, 2004). However, more likely, these indicators may be the consequence of the low fraction melting proposed for the HITIS parental magma. This notion is supported by the discussion given earlier under the heading "Parental magma".

The Ir/Pd ratio for the HITIS is high which, based on the data compiled by Maier and Barnes (2004), is indicative of alkali basalt (Figure 13).

Sulphur assimilation

With the exception of the BGU of Uitkomst Complex, the sulphur isotopic data clusters close to 0 permil, which is a mantle signature and suggests negligible contamination with sulphur from the country rock. This statement assumes that the country rock in all instances had isotopic ratios significantly different from that of the primary magmatic zero permil values, an

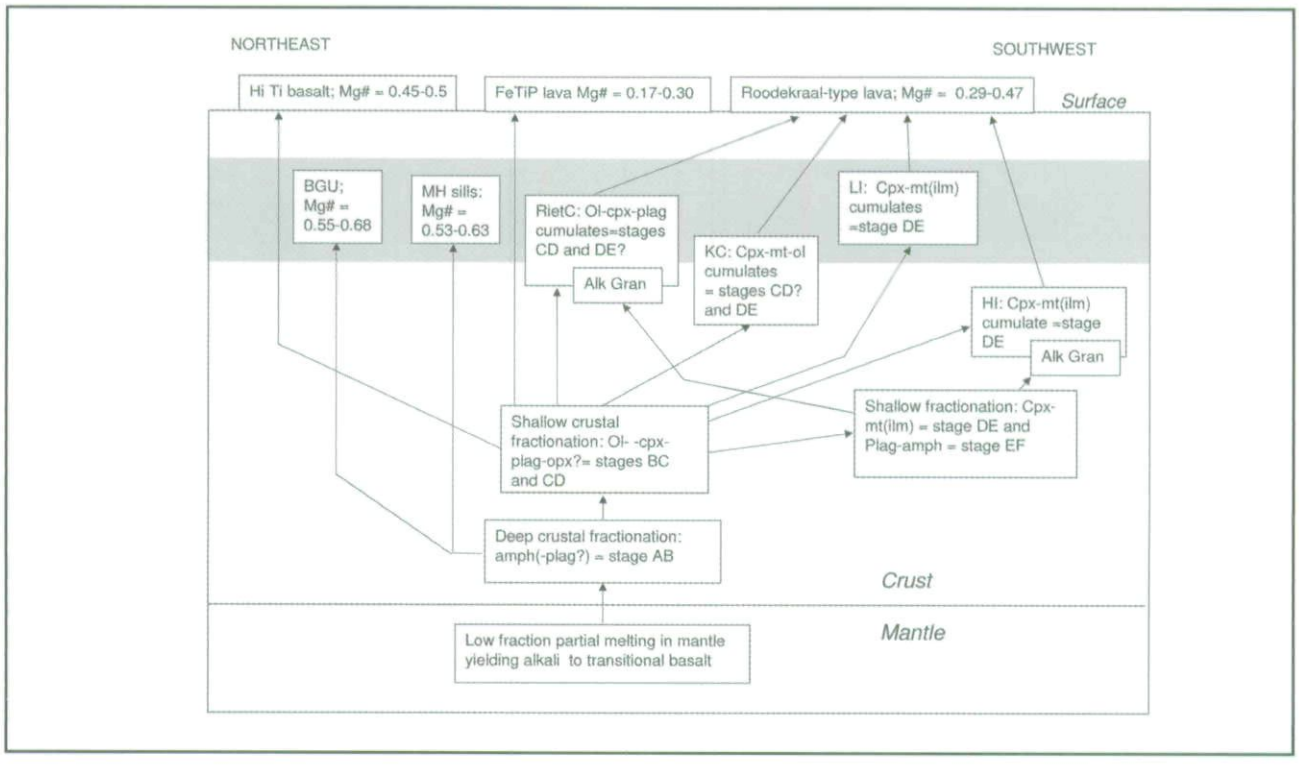

Figure 20. Petrological model for the HITIS rocks. The horizontal grey band represents the Malmani Subgroup (dolomite).

assumption that may be valid for the metasedimentary rocks of both the Transvaal Supergroup (Cameron, 1982) and the Witwatersrand Supergroup (England *et al.*, 2002).

Metamorphism

Gibson and Wallmach (1995) reported a high geothermal gradient (~40°C/km) in the Vredefort area at the time before the Vredefort impact event at 2023 Ma (Kamo *et al.*, 1996). High heat flow patterns have also been postulated for the Witwatersrand basin (Schreyer and Bisshoff, 1982; Wallmach and Meyer, 1990) in general. The relative abundance of HITIS bodies in the relevant area raises the possibility that their emplacement at supracrustal levels is to a large extent responsible for this observed heat flow pattern, as also earlier proposed by De Waal and Armstrong (2000) and Graham *et al.*, 2005).

Conclusion

A high-Ti igneous suite of mafic to felsic igneous rocks (acronym: HITIS) was emplaced at ca. 2055 Ma as km-sized bodies in an area of 20 000 km^2, bounded roughly by a quadrangle confined between Marble Hall, Badplaas, Parys and Potchefstroom, South Africa. The suite includes the Marble Hall sills and related breccia, the Basal Gabbro Unit of the Uitkomst Complex, the Lindeques Drift and Heidelberg Intrusions, the volcanic Roodekraal Complex, the Rietfontein Complex, the Koedoesfontein Complex, the Schoongezicht Complex, the Vredefort alkali granite, as well as the high-Ti basalt and FeTiP basaltic lava of the Rooiberg Group.

The most primitive HITIS magma, the Bu magma, was transitional to alkali basaltic in nature and enriched in volatiles. It represents a low fraction mantle melt that was produced from the same source that yielded the Bushveld B3-type magma. This Bu magma underwent deep-seated (lower crustal?) amphibole fractionation. Intermittent extractions from the magma chamber(s) were emplaced at Uitkomst to form the chill zone of the Basal Gabbro Unit, and at Marble Hall the diorite sill complex. At Uitkomst the magma was enriched in copper, hence the copper-rich character of the disseminated sulphide in the Basal Gabbro Unit, whereas at Marble Hall copper mineralization is less well developed.

In addition to gabbroid rocks that represent liquid fractions, olivine, clinopyroxene and/or clinopyroxene-plagioclase cumulates derived from these magmas are also locally developed at Marble Hall and at Uitkomst. Breccias representing explosive release of volatiles are developed at Marble Hall.

Subsequent shallow-level crustal fractionation raised the Fe content of the residual magma to produce a ferrobasaltic magma, which is parental to the Schoongezicht Complex, the Rietfontein Complex, the Lindeques Drift and Heidelberg Intrusions, as well as the volcanic Roodekraal Complex, and which gave rise to an array of clinopyroxene±magnetite (-ilmenite)±olivine±plagioclase cumulates (*i.e.* spessartite, magnetite-clinopyroxenite, wehrlite, troctolite, magnetite dunite, magnetite websterite). Marked copper enrichment is present in the Lindeques Drift and Heidelberg Intrusions and the Schoongezicht Complex. With continued shallow-level fractionation

the magnetite(-ilmenite)-to-clinopyroxene ratio of the fractionating solid increased causing extreme depletion of Fe and strong enrichment of Na and Al in the residual liquid. In the final stage of differentiation, dominantly sodic plagioclase precipitated from the melt to produce a residual liquid with the composition of the Vredefort alkali granite. The latter is estimated to represent the final 3% of residual liquid of the original HITIS parental magma.

Intermittent tappings from the fractionating magma chambers at various stages of development extruded as the high-Ti basalt and FeTiP lava of the Rooiberg Group and the mugearite lava of the Roodekraal Complex. The possible existence at 2055 Ma before present of an active volcanic field to the south of the current Bushveld outcrops is indicated.

The HITIS rocks typically contain sub-economic disseminated copper sulphide segregations. In the Roodekraal Complex, this mineralization is concentrated along faults and contact zones and is hydrothermally overprinted with secondary CuFe sulphide.

Acknowledgements

The authors are indebted to Rina White (drafting), Maggi Laubser (XRF), Sabine Verryn (XRD), Peter Graeser (EMP), Marko Claassen (thin section laboratory) and Peter Sibiya (thin section laboratory) of the University of Pretoria and Andreas Spath (ICP-MS) of the University of Cape Town for long-standing and excellent technical and analytical support. Sarah-Jane Barnes is sincerely thanked for PGE-analyses on selected samples. Financial support from the Foundation for Research Development and THRIP, through the Center for Research on Magmatic Ore Deposits, is gratefully acknowledged. We also thank W.D. Maier and M. Cloete for their constructive reviews of the paper. All remaining discrepancies that may have crept through are the sole responsibility of the first author.

References

Agranier, A. (2000). Petrological and geochemical study of the chilled margin of the Uitkomst intrusion, South Africa. *Unpublished BSc Research Report, Joseph Fourrier University, France.* 31pp.

Anonymous. (1997). Nkomati - South Africa's First Primary Nickel Mine. *South African Mining Coal, Gold and Base Minerals*, July, 27-31.

Armstrong, R.A., Compston, W., Retief, E.A., Williams, L.S. and Welke, H.J. (1991). Zircon ion microprobe studies bearing on the age and evolution of the Witwatersrand basin. *Precambrian Research*, **53**, 243-266.

Babayeju, O.K.T. (1999). Geophysical investigation of the Marble Hall fragment of the Bushveld Complex. *Unpublished MSc dissertation, University of Pretoria, South Africa.* 100pp.

Beccaluva, L., Siena, F., Coltort, M., Di Grande, A., Lo Guidice, A., Macciotta, G., Tassinari, R. and Vaccaro, C. (1998). Nephelinitic to tholeiitic magma generation in a transitional tectonic setting: an integrated model for the Iblean volcanism, Sicily. *Journal of Petrology*, **39**, 1547-1576.

Bedard, J.H. (1994). A procedure for calculating the equilibrium distribution of trace elements among the minerals of cumulate rocks, and the concentration of trace elements in coexisting liquids. *Chemical Geology*, **118**, 143-153.

Bédard, L.P. and Barnes, S.-J. (2002). A comparison of the capacity of FA-ICP-MS and FA-INAA to determine platinum-group elements and gold in geological samples. *Journal of Radioanalytical and Nuclear Chemistry*, **254**, 319-329

Bennett, H., and Oliver, G. (1992) XRF Analysis of Ceramics, Minerals and Applied Materials. *John Wiley and Sons, West Sussex, United Kingdom*, 298 pp.

Bisschoff, A.A. (1969). The petrology of the igneous and metamorphic rocks in the Vredefort Dome and adjoining parts of the Potchefstroom syncline. *Unpublished DSc thesis, University of Pretoria, South Africa.* 243pp.

Bisschoff, A.A. (1972). The dioritic rocks of the Vredefort dome. *Transactions of the Geological Society of South Africa*, **75**, 31-45.

Bisschoff, A.A. (1999). Vredefort Dome. Explanation of geological sheets 2627CA, CB, CC, CD, DA, DC and 2727AA, AB, BA (1:50000). Pretoria, *Council for Geoscience, South Africa.* 49 pp.

Burger, A.J. and Coertze, F.J. (1975). Age determinations – April 1972 to March 1974. *Annals of the Geological Survey of South Africa*, **10**, 135-141.

Cameron, E.M. (1982). Sulphate and sulphate reduction in early Precambrian oceans. *Nature*, **296**, 145-148.

Cawthorn, G.R., Davies, G., Clubley-Armstrong, A. and McCarthey, T.S. (1981). Sills associated with the Bushveld Complex, South Africa: an estimate of the parental magma composition. *Lithos*, **14**, 1-16.

Cheney, E. and Twist, D. (1991). The conformable emplacement of the Bushveld mafic rocks along a regional unconformity in the Transvaal succession of South Africa. *Precambrian Research*, **52**, 115-132.

Clark, R.J.McH. (1972). The geology of the Roodekraal Igneous Complex. Potchefstroom District. *Unpublished MSc dissertation, University of the Witwatersrand, Johannesburg, South Africa*, 137pp.

Cox, K.G., Bell, J.D. and Pankhurst, R.J. (1979). The interpretation of igneous rocks. *George, Allen and Unwin, London, United Kingdom*, 450pp.

Curl, E.A. (2001) Parental magma of the Bushveld Complex, South Africa. *Unpublished PhD thesis, Monash University, Victoria, Australia.* 140pp.

Davies, G. and Cawthorn, R.G. (1984). Mineralogical data on a multiple intrusion in the Rustenburg Layered Suite of the Bushveld Complex. *Mineralogical Magazine*, **48**, 439-448.

Davies, G. and Tredoux, M. (1985). The Platinum- Group Element and Gold Contents of the Marginal Rocks and Sills of the Bushveld Complex. *Economic Geology*, **80**, 838-848.

Davies, G., Cawthorn, R.G., Barton, J.M. and Morton, M. (1980). Parental magma to the Bushveld Complex. *Nature*, **287**, 33-35.

De Waal, S.A. (1963) Die plooikompleks van die Sisteem Transvaal noord van Marble Hall en die meegaande metamorfe en intrusiegesteentes. *Unpublished MSc dissertation, University of Pretoria, South Africa.* 86pp.

De Waal, S.A. (1969) Interference folding of Bushveld-Igneous-Complex age in the Transvaal System north of Marble Hall, Transvaal. *In:* D.J.L. Visser and G. Von Gruenewaldt (Editors), Symposium on the Bushveld Igneous Complex and other layered intrusions. *Special Publication of the Geological Society of South Africa*, **1**, 283-288.

De Waal, S.A., and Armstrong, R.A. (2000). The age of the Marble Hall diorite, its relationship to the Uitkomst Complex, and evidence for a new magma type associated with the Bushveld igneous event. *South African Journal of Geology*, **103**, 128-140.

De Waal, S.A. and Gauert, C.D.K. (1997). The Basal Gabbro Unit and the identity of the parental magma of the Uitkomst Complex, Badplaas, South Africa. *South African Journal of Geology*, **100**, 349-362.

De Waal, S.A., Graham, I.T. and Armstrong, R.A. (2005). The Lindeques Drift and Heidelberg Intrusions and the Roodekraal Complex, Vredefort, South Africa: comagmatic plutonic and volcanic products of a 2055 Ma ferrobasaltic magma. *South African Journal of Geology*, **109**, 279-300.

De Waal, S.A., Graham, I.T., and Phillips, D. (2002). Age and significance of the Marble Hall breccia, Bushveld Complex, South Africa. *South African Journal of Geology*, **105**, 227-240.

De Waal, S.A., Maier, W.D., Armstrong, R.A. and Gauert, C.D.K. (2001). The age and parental magma of the Uitkomst Complex. *Canadian Mineralogist*, **39**, 557-571.

De Waal , S.A. and Theart, H.F.J. (2004). Amphibole(-plagioclase) fractionation in the high-Ti parental magma of the Basal Gabbro Unit, Uitkomst Complex, and the implications for the associated sulphide mineralization. *Geoscience Africa 2004, Abstract Volume, Geological Society of South Africa*, 160-161.

Eales, C.V. (2002). Caveats in defining the magma parental to the mafic rocks of the Bushveld Complex, and the manner of their emplacement: review and commentary. *Mineralogical Magazine*, **66**, 815-832.

Elsenbroek, J.H. (1991). Die struktuur en petrologie van die alkaligraniet in die Vredefortkoepel noordwes van Parys. *Unpublished MSc dissertation, Potchefstroom University, South Africa*. 105pp.

Elsenbroek, J.H. (1993). Die struktuur en petrologie van die alkaligraniet in die Vredefortkoepel noordwes van Parys. *Bulletin of the Geological Survey of South Africa*, **110**, 63pp.

England, G.L., Rasmussen, B., Krapez, B. and Groves, D.I. (2002). Palaeoenvironmental significance of rounded pyrite in siliciclastic sequences of the Late Archaean Witwatersrand Basin: oxygen-deficient atmosphere or hydrothermal alteration? *Sedimentology*, **49**, 1133-1156.

Floyd, P.A. and Winchester, J.A. (1975). Magma-type and tectonic setting discrimination using immobile elements. *Earth and Planetary Science Letters*, **27**, 211-218.

Frick, C. (1975.) The geology and petrology of the Kaffirskraal igneous complex. *Transactions of the Geological Society of South Africa*, **78**, 11-23.

Frick, C. (1979). Geology, mineralogy and petrology of the Kaffirskraal Complex. *Bulletin of the Geological Survey of South Africa*, **64**, 42pp.

Gauert, C.D.K. (1998): The Petrogenesis Of The Uitkomst Complex, Mpumalanga Province, South Africa. *Unpublished PhD Thesis, University of Pretoria, South Africa*, 314pp.

Gauert, C.D.K., de Waal, S.A. and Wallmach, T. (1995). Geology of the ultrabasic to basic Uitkomst complex, eastern Transvaal, South Africa: an overview. *Journal of African Earth Sciences*, **21**, 553-570.

Gauert, C.D.K., Jordaan, L.J., De Waal, S.A. and Wallmach, T. (1996). Isotopic constraints on the source of S for the base metal sulfides of the Uitkomst Complex, Badplaas, South Africa. *South African Journal of Geology*, **99**, 41-50.

Gibson, R.L., and Reimold, W.U. (2001). The Vredefort impact structure: the scientific evidence and a two-day excursion guide. *Memoir of the Council for Geoscience, South Africa*, **92**, 111pp.

Gibson, R.L. and Wallmach, T. (1995). Low pressure-high temperature metamorphism in the Vredefort Dome, South Africa – anticlockwise pressure-temperature path followed by rapid decompression. *Geological Journal*, **30**, 319-331.

Gomwe, T.E.S (2002). A geochemical profile of the Uitkomst Complex in the farm Slaaihoek, with special reference to the platinum-group elements and Sm-Nd isotopes. *Unpublished MSc dissertation, University of Pretoria, South Africa*. 97 pp and 2 appendices.

Graham, I.T., De Waal, S.A. and Armstrong, R.A. (2005). New U-Pb SHRIMP zircon age for the Schurwedraai alkali granite: implications for pre-impact development of the Vredefort Dome and extent of Bushveld magmatism, South Africa. *Journal of African Earth Sciences*, **43**, 537-548.

Green, D.H. (1982). Anatexis of mafic crust and high pressure crystallization of andesite. *In:* R. S. Thorpe (Editor), Andesites. *John Wiley and Sons, New York, United States of America*, 465-488.

Harmer, R.E. and Sharpe, M.R. (1985). Field relations and strontium isotope systematics of the marginal rocks of the eastern Bushveld Complex. *Economic Geology*, **80**, 813-837.

Hattingh, P.J. (1980). The structure of the Bushveld Complex in the Groblersdal-Lydenburg-Belfast area of the eastern Transvaal as interpreted from regional gravity sources. *Transactions of the Geological Society of South Africa*, **83**, 125-133.

Hatton, C.J. (1988). Densities and liquidus temperatures of Bushveld parental magmas as constraints on the formation of the Merensky Reef in the Bushveld Complex, South Africa. *In:* M. D. Prendergast and M. J. Jones (Editors), Magmatic Sulphides: the Zimbabwean Volume. *Institute of Mining and Metallurgy, London, United Kingdom*, 87-93.

Hornsey, R.A. (1999) The genesis and evolution of the Nkomati Ni-sulphide deposit, Mpumalanga Province, South Africa. *Unpublished MSc dissertation, University of Natal, South Africa*. 224pp.

Kamo, S.L., Reimold, W.U., Krogh, T.E. and Colliston, W.P. (1996). A 2.023 Ga age for the Vredefort impact event and a first report of shock metamorphosed zircons in pseudotachylitic breccias and granophyre. *Earth and Planetary Science Letters*, **144**, 369-388.

Kruger, F.J. (1994). The Sr-isotopic stratigraphy of the western Bushveld Complex. *South African Journal of Geology*, **97**, 393-398.

Le Bas, M.J. (1962). The role of aluminium in igneous clinopyroxene with relation to their parentage. *American Journal of Science*, **260**, 267-288.

Maaloe, S. and Aoki, K. (1977). The major element compositions of the upper mantle estimated from the composition of lherzolites. *Contributions to Mineralogy and Petrology*, **63**, 161-173.

Maier, W.D. and Barnes, S.-J. (2004). Pt/Pd and Pd/Ir ratios of mantle-derived magmas: A possible role for mantle metasomatism. *South African Journal of Geology*, **107**, 333-340.

Maier, W. D., Gomwe, T., Barnes , S.-J., Li, C. and Theart, H. (2004). Platinum Group Elements in the Uitkomst Complex, South Africa. *Economic Geology*, 99, 499-516.

Nel, L.T. and Jansen, H. (1957). The geology of the country around Vereeniging. *Geological Survey of South Africa, Explanation of the geological map sheet 62*, 90pp.

Pearce, J.A. and Norry, M.J. (1979). Petrogenetic implications of Ti, Zr, Y, and Nb variations in volcanic rocks. *Contributions to Mineralogy and Petrology*, **69**, 33-47.

Roeder, P.L. and Emslie, R.F. (1970). Olivine-Liquid Equilibrium. *Contributions to Mineralogy and Petrology*, **29**, 275-289.

Rogers, A.W. (1922). The geology of the country around Heidelberg. *Special publication of the Geological Survey of South Africa*, **4**, 81pp.

Rollinson, H. (1993). Using geochemical data: evaluation, presentation, interpretation. *Longman Scientific and Technical, Harlow, United Kingdom*, 352pp.

Schreyer, W. and Bisschoff, A.A. (1982). Kyanite as a metamorphic mineral in the Witwatersrand sediments at Johannesburg and Krugersdorp, South Africa. *Transactions of the Geological Society of South Africa*, **85**, 211-214.

Schweitzer, J.-K. (1998). The Dullstroom Formation and the Rooiberg Group, volcanic rocks associated with the Bushveld Complex. *Unpublished PhD thesis, University of Pretoria, South Africa*. 20pp + 10 Appendices.

Schweitzer, J.-K., Hatton, C.J. and De Waal, S.A. (1995). Regional lithochemical stratigraphy of the Rooiberg Group, upper Transvaal Supergroup: A proposed new subdivision. *South African Journal of Geology*, **98**, 245-255.

Sharpe, M.R. (1981): The Chronology Of Magma Influxes To The Eastern Compartment, Bushveld Complex, As Exemplified By Its Marginal Border Groups. *Journal of the Geological Society, London*, **138**, 307-326.

Sharpe, M.R. (1984). Petrography, classification, and chronology of mafic sill intrusions beneath the eastern Bushveld Complex. *Geological Survey of South Africa Bulletin* **77**, 34pp.

Sharpe, M.R. (1985). Strontium Isotope Evidence For Preserved Density Stratification In The Main Zone Of The Bushveld Complex, South Africa. *Nature*, **316**, 119-126.

Shervais, J.W. (1982). Ti-V plots and the petrogenesis of modern and ophiolitic lavas. *Earth and Planetary Science Letters*, **59**, 101-118.

Snyman, C.P. (1958). 'n Gneiss, 'n koepelstruktuur en die metamorfose van die Sisteem Transvaal suid van Marble Hall, Transvaal. *Transactions of the Geological Society of South Africa*, **61**, 225-262.

Strauss, T.A.L. (1995). Petrography and geochemistry of the Basal Gabbro Unit, Uitkomst Complex. *Unpublished MSc dissertation, Rhodes University, South Africa*. 103pp.

Van Zyl, A.M. (1996) The sulphides of the Uitkomst Complex, Badplaas, South Africa. *Unpublished MSc dissertation, University of Pretoria, South Africa*. 121pp.

Wallmach, T. and Meyer, F.M. (1990). A petrogenetic grid for metamorphosed aluminous Witwatersrand shales. *South African Journal of Geology*, **93**, 93-102.

Walraven, F., (1997). Geochronology of the Rooiberg Group, Transvaal Supergroup, South Africa. *University of the Witwatersrand, South Africa, Economic Geology Research Unit Information Circular* **31**, 1-28.

Walraven, F., Hattingh, E. (1993). Geochronology of the Nebo Granite, Bushveld Complex. *South African Journal of Geology*, **96**, 31-41.

Walraven, F. and Martini, J. (1995). Zircon Pb-evaporation age determinations of the Oak Tree Formation, Chuniespoort Group, Transvaal Sequence: implications for Transvaal-Griqualand West basin correlations. *South African Journal of Geology*, **98**, 58-67.

Watson, J.S. (1996). Fast, simple method of powder pellet preparation for X-Ray fluorescence analysis. *X-Ray Spectrometry*, **25**, 173-174.

Winchester, J.A. and Floyd, P.A. (1976). Geochemical magma type discrimination; application to altered and metamorphosed basic igneous rocks. *Earth and Planetary Science Letters*, **28**, 459-466.

Editorial handling: Adam Bumby